

1

2

3

Supplementary Information

4

5 **Molecular Basis of Regio- and Stereo-Specificity in**

6 **Biosynthesis of Bacterial Heterodimeric Diketopiperazines**

7

8

9

Sun *et al.*

10

Table of Contents

11

12

13 1. Supplementary Figures

14 **Supplementary Fig. 1.** Spectra of compound NAS-B

15 **Supplementary Fig. 2.** Key HMBC and ROESY correlations observed in NAS-B,
16 ASP-A and NAS-E.

17 **Supplementary Fig. 3.** Spectra of compound ASP-A

18 **Supplementary Fig. 4.** HPLC analysis of enzymatic conversion of cW_L-P_L by
19 mutants in the N-terminal part of NasF₅₀₅₃ and NascB.

20 **Supplementary Fig. 5.** The eight fragments in the C-terminal part of NascB

21 **Supplementary Fig. 6.** HPLC analysis of enzymatic conversion of cW_L-P_L by
22 mutants on the C-terminal part of NascB.

23 **Supplementary Fig. 7.** HPLC analysis of enzymatic conversion of cW_L-P_L by
24 mutants of NascB in fragment-7.

25 **Supplementary Fig. 8.** HPLC analysis of the Nas_{F5053} mutants which can improve
26 the production of NAS-B.

27 **Supplementary Fig. 9.** Spectra of compound NAS-E

28 **Supplementary Fig. 10.** Spectra of the synthetic NAS-E (TM-3)

29 **Supplementary Fig. 11.** Crystal structure of Nas_{F5053}.

30 **Supplementary Fig. 12.** Superposition of Nas_{F5053} without the substrates (cyan) and
31 with the substrates (orange).

32 **Supplementary Fig. 13.** UV-Vis titration and determination of the binding constants
33 of cW_L-P_L to Nas_{F5053} (A-C), Nas_{F5053}-Q65I-A86G (D-F) and Nas_{F5053}-S284A-V288A
34 (G-I).

35 **Supplementary Fig. 14.** RMSD variation in molecular dynamics simulations.

36 **Supplementary Fig. 15.** SDS-PAGE analysis of recombinant proteins.

37

38 2. Supplementary Tables

39 **Supplementary Table 1.** Product profiles and yields of the P450 reactions using

40 cW_L-P_L as substrate (NasB, NasbB, NascB, Nas_{F5053} and AspB).

41 **Supplementary Table 2.** NMR data of compound NAS-B in DMSO-*d*₆.

42 **Supplementary Table 3.** NMR data of compound ASP-A in DMSO-*d*₆.

43 **Supplementary Table 4.** NMR data of compound NAS-E in DMSO-*d*₆.

44 **Supplementary Table 5.** X-ray data collection and structure refinement statistics for
45 Nas_{F5053} and its mutants.

46 **Supplementary Table 6.** Bacterial strains and plasmids.

47 **Supplementary Table 7.** Primers used in this study.

48

49 **3. Supplementary Methods**

50 3.1. General materials and methods

51 3.2. Cloning, expression, and purification of P450s and associated proteins

52 3.3. P450 enzyme assays

53 3.4. Scaled catalytic reaction and purification of compounds NAS-B and ASP-A

54 3.5. Site-directed mutagenesis of Nas_{F5053} and NascB

55 3.6. Construction and screening of Nas_{F5053} mutant libraries

56 3.7. Synthesis of NAS-E

57 3.8. Cloning, expression, crystallization and crystal structure determination of
58 Nas_{F5053} and its mutants

59 3.9. Molecular dynamics simulations

60 3.10. UV-Vis titration and determination of the binding constants of cW_L-P_L to Nas_{F5053},

61 Nas_{F5053}-Q65I-A86G or Nas_{F5053}-S284A-V288A.

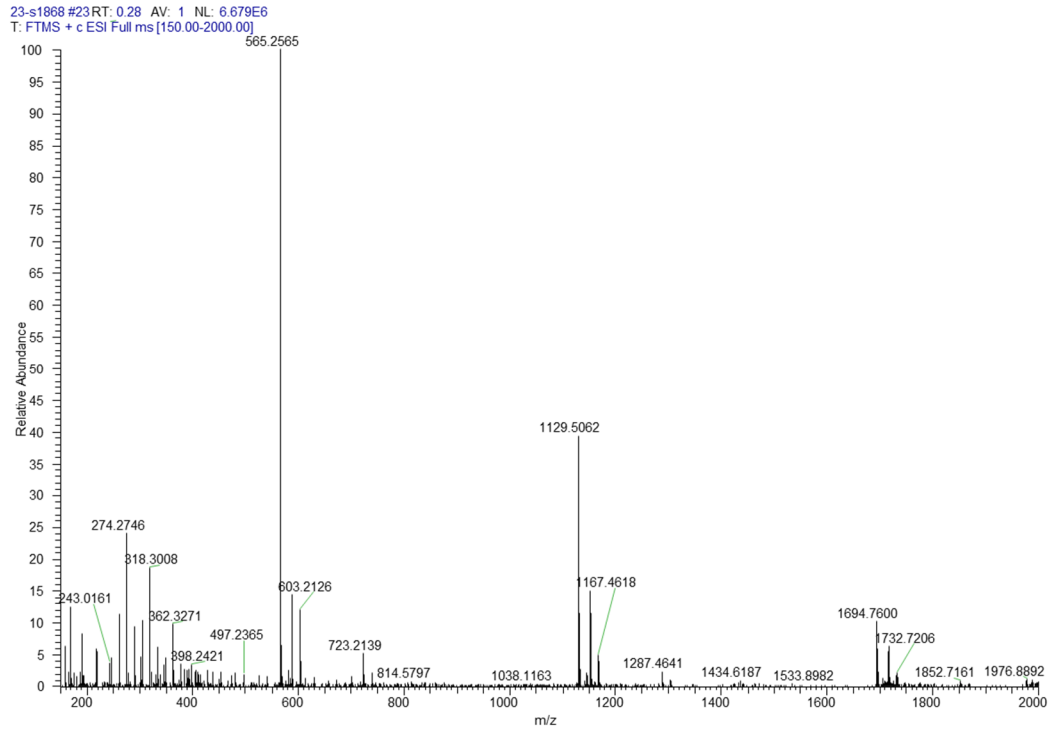
62

63 **4. Supplementary References**

64

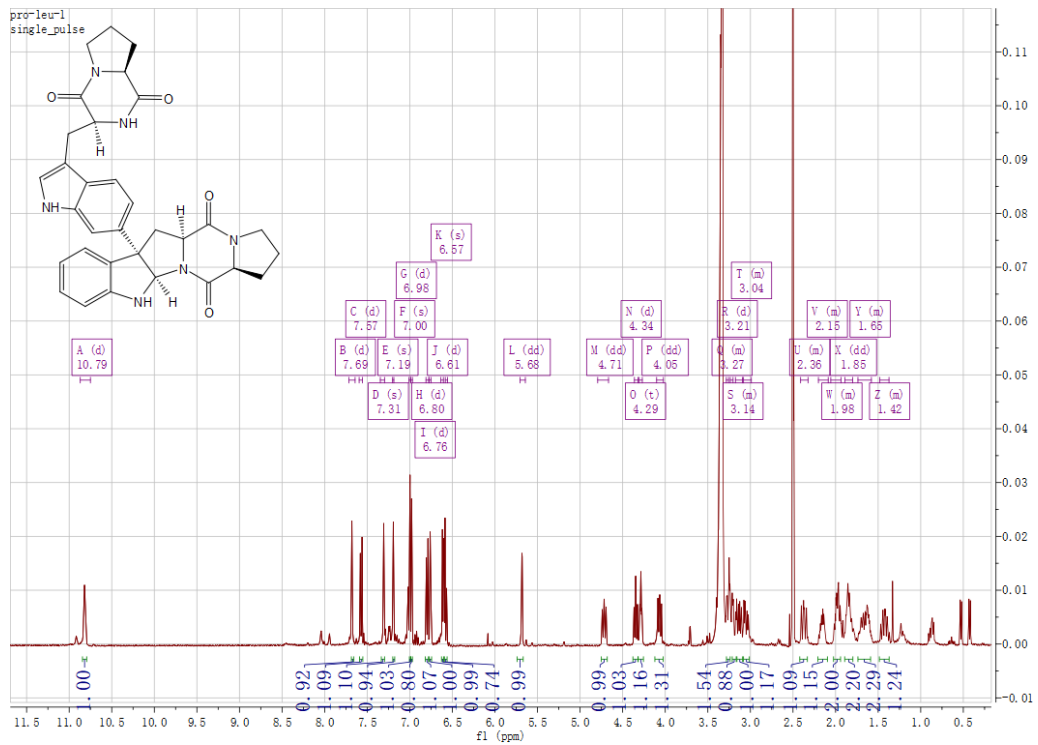
65 **1. Supplementary Figures**

66 **a**



67

68 **b**



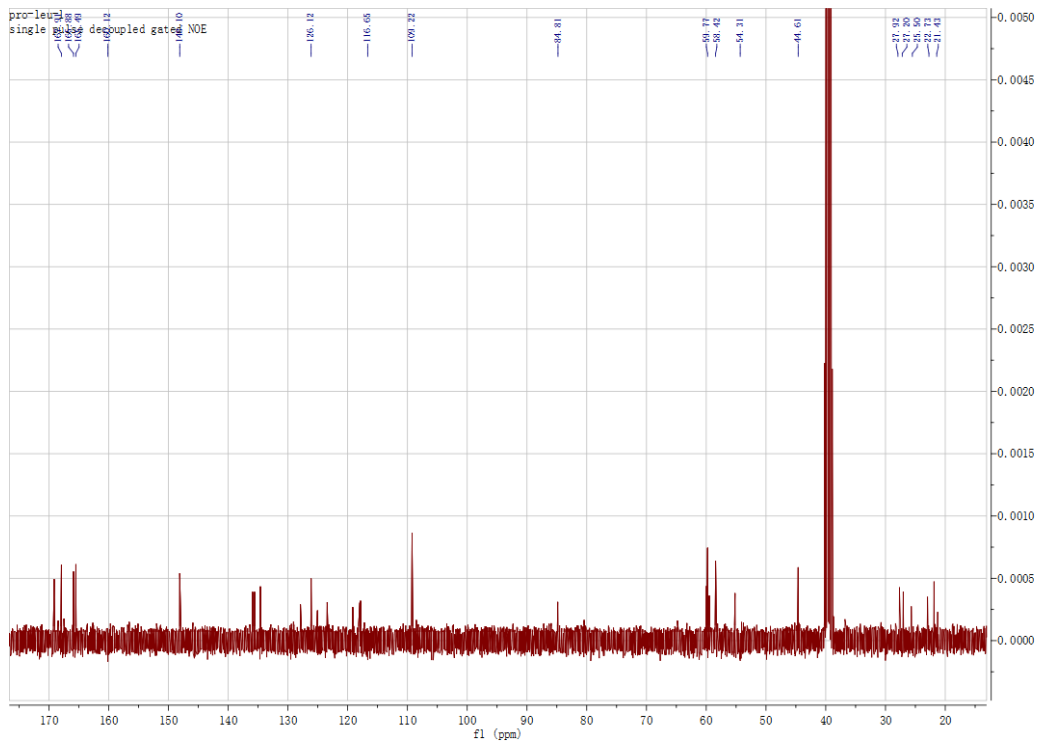
69

70

71

72

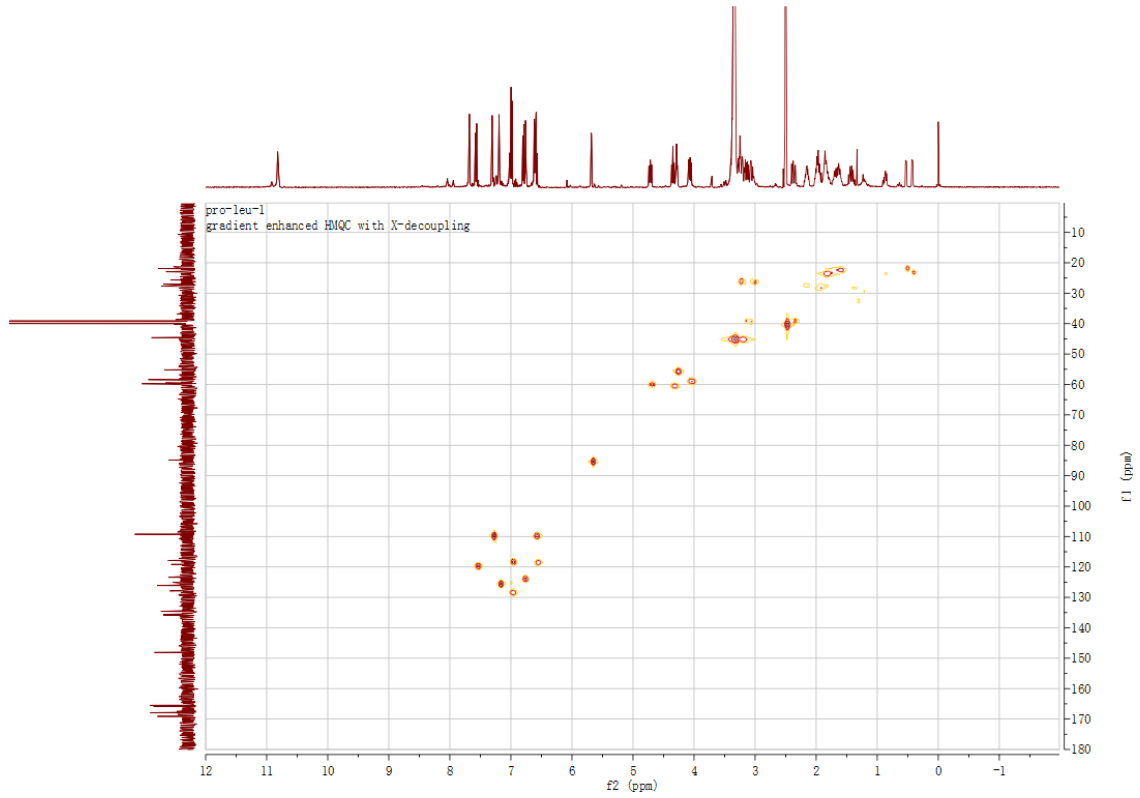
73 **c**



74

75

76 **d**

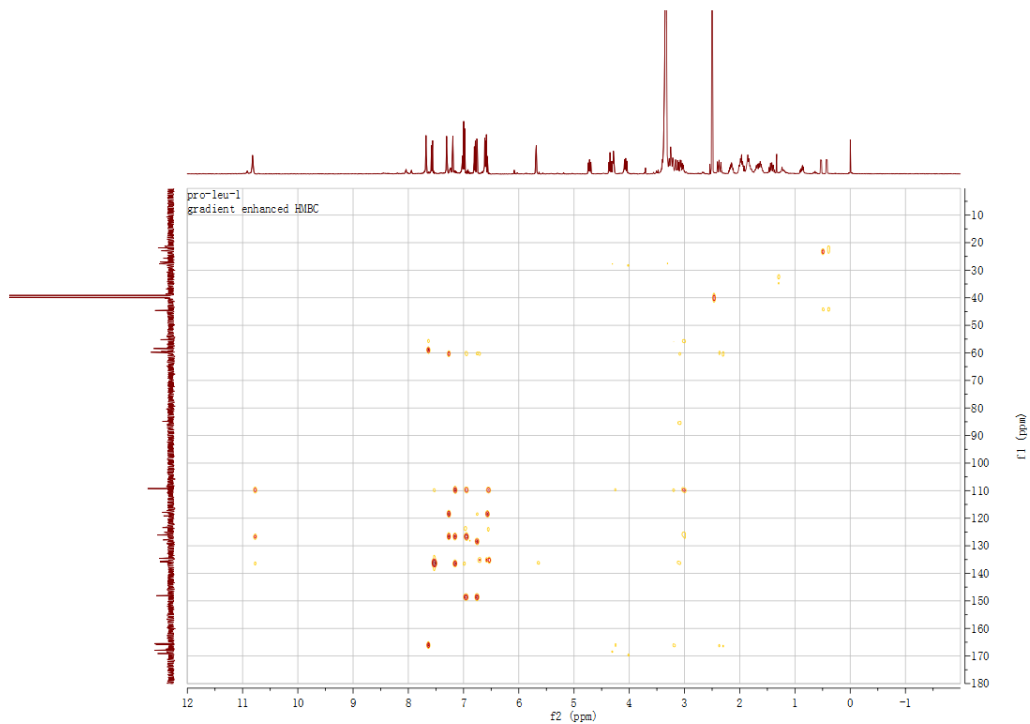


77

78

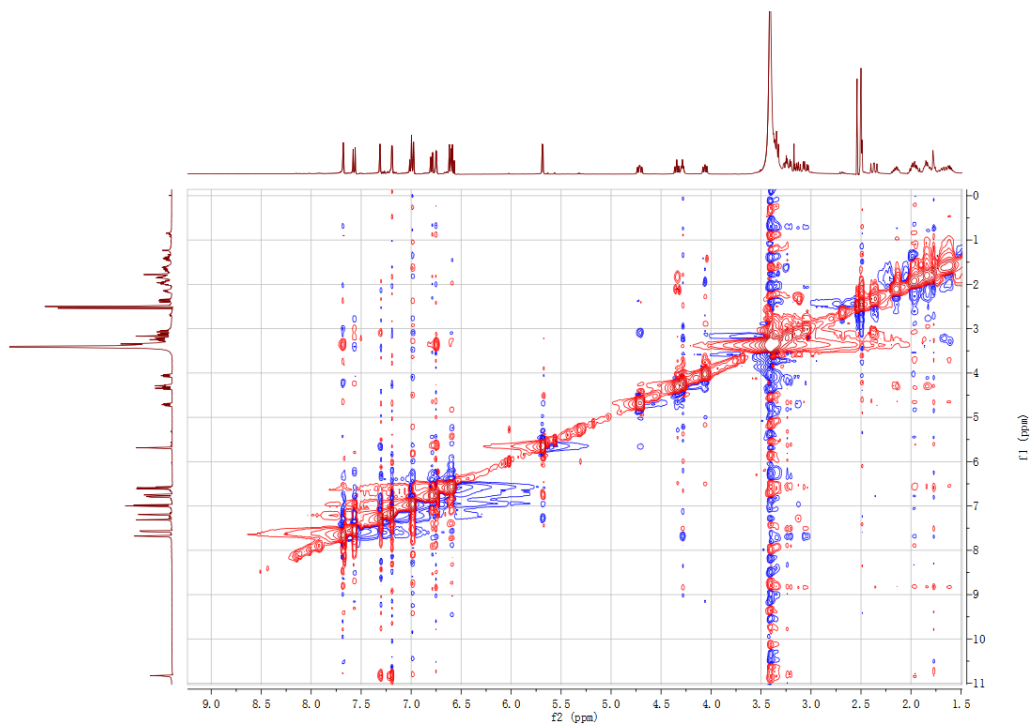
79

80 e



81

82 f

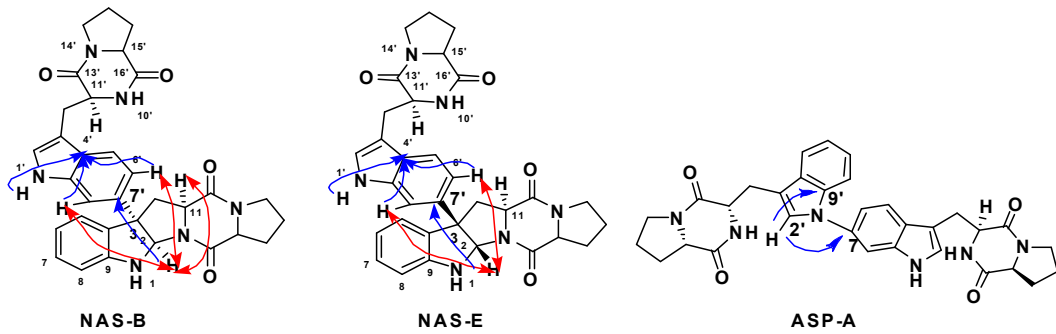


83

84 **Supplementary Fig. 1.** Spectra of compound NAS-B. (a) HRESIMS of compound of
85 NAS-B (b) ^1H NMR of compound of NAS-B (c) ^{13}C NMR of compound of NAS-B (d)
86 HSQC of compound of NAS-B (e) HMBC of compound of NAS-B (f) ROSEY of
87 compound of NAS-B.

88

89



90

91

92 **Supplementary Fig. 2.** Key HMBC and ROESY correlations observed in NAS-B, ASP-

93 A and NAS-E. (HMBC: blue; ROESY: red).

94

95

96

97

98

99

100

101

102

103

104

105

106

107

108

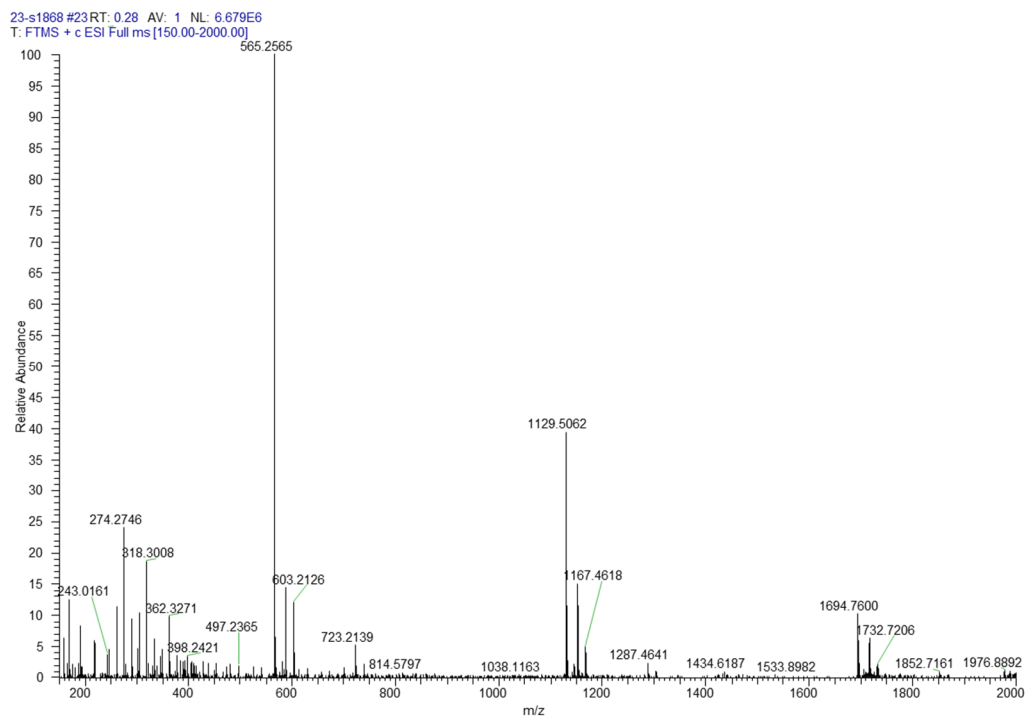
109

110

111

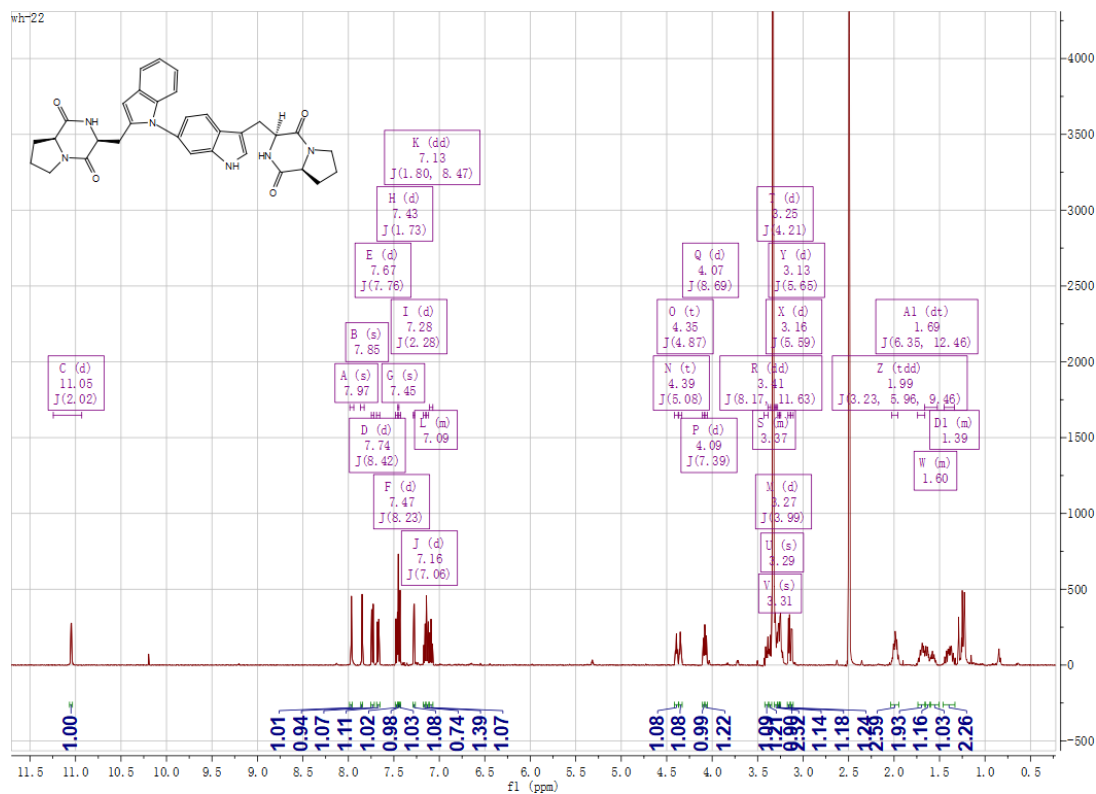
112

113 a



114

115 b



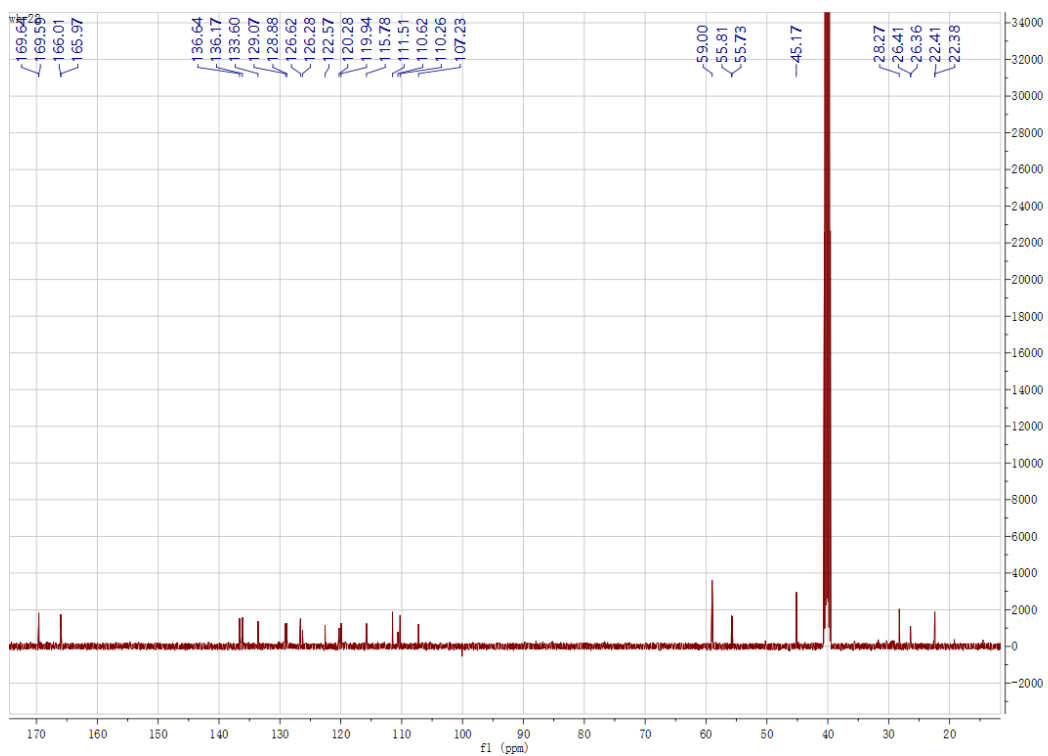
116

117

118

119

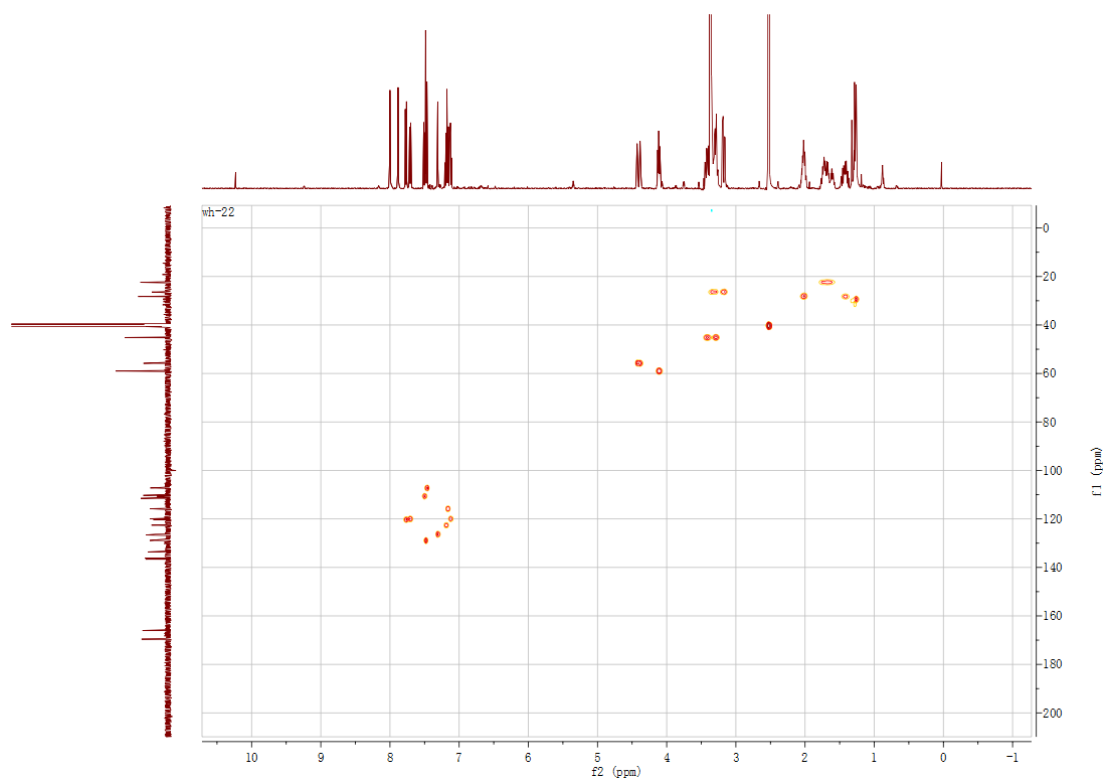
120 **c**



121

122

123 **d**

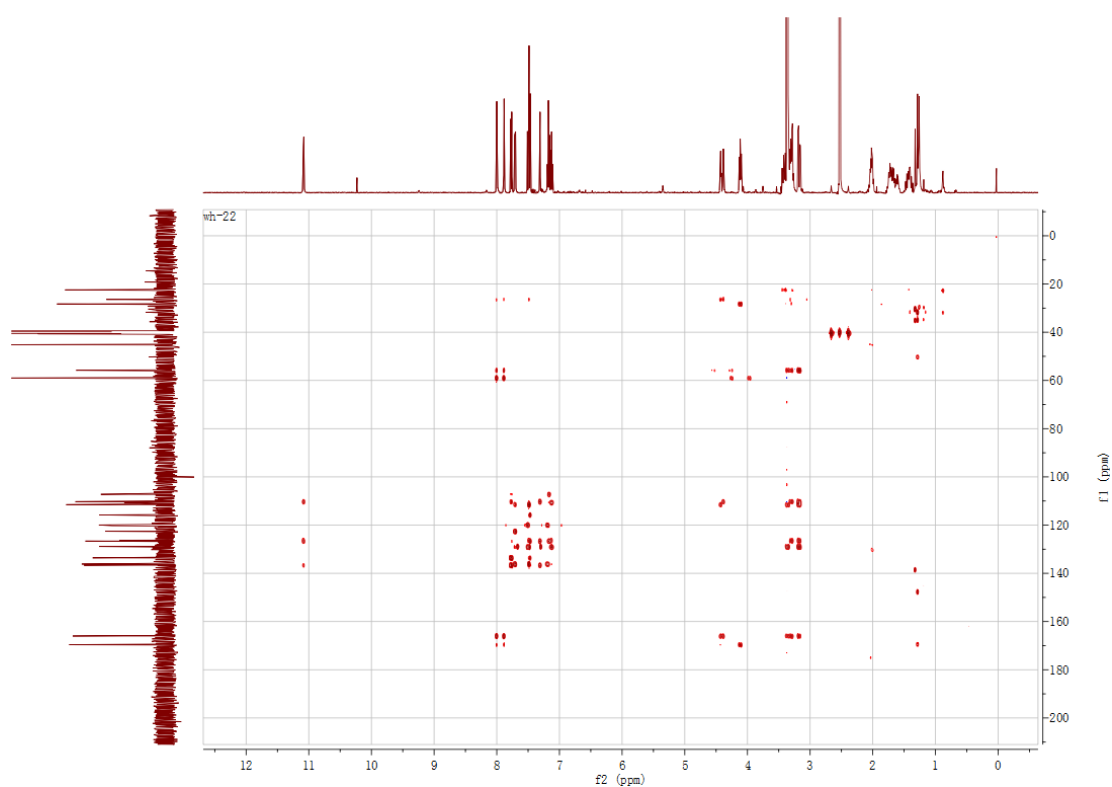


124

125

126

127 e



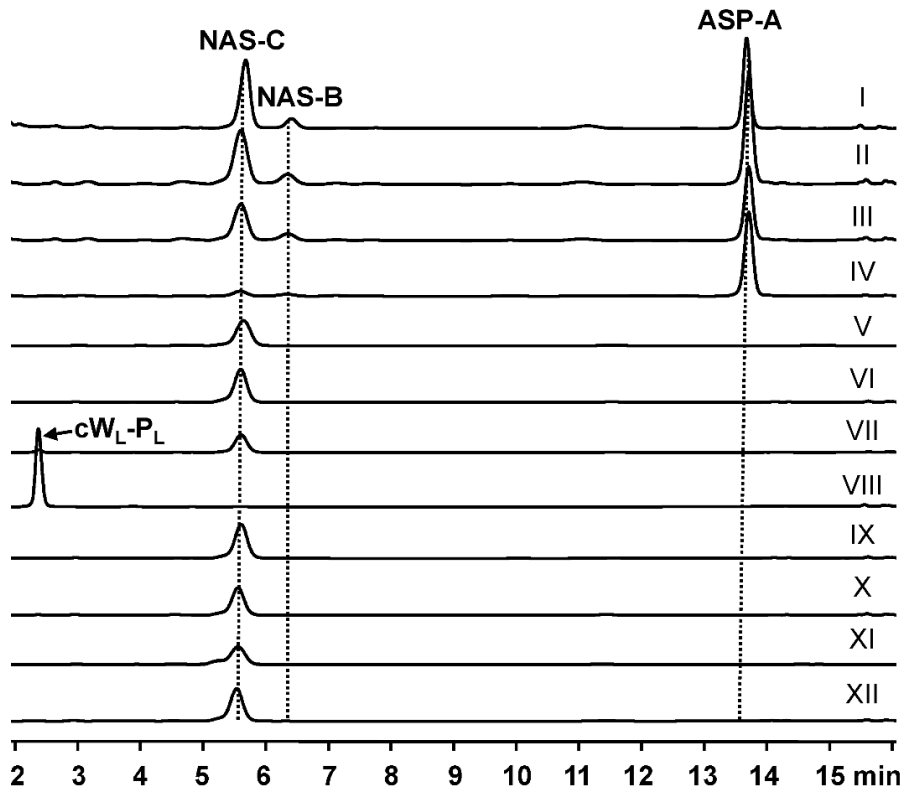
128

129

130 **Supplementary Fig. 3.** Spectra of compound ASP-A. (a) HRESIMS of compound of
131 ASP-A; (b) ^1H NMR of compound of ASP-A; (c) ^{13}C NMR of compound of ASP-A ; (d)
132 HSQC of compound of ASP-A; (e) HMBC of compound of ASP-A.

133

134



135

136 **Supplementary Fig. 4.** HPLC analysis of enzymatic conversion of cW_L-P_L by mutants

137 in the N-terminal part of Nas_{F5053} and $NascB$. I) Nas_{F5053} -P43A-T49A-K52E; II) Nas_{F5053} -

138 I87V; III) Nas_{F5053} -G84A; IV) Nas_{F5053} -P43A-T49A-K52E-G84A; V) $NascB$ -P40H; VI)

139 $NascB$ -V44A; VII) $NascB$ -T49A; VIII) $NascB$ -K52E; IX) $NascB$ -S67F; X) $NascB$ -F62L;

140 XI) $NascB$ -G84A; XII) $NascB$ -I87V.

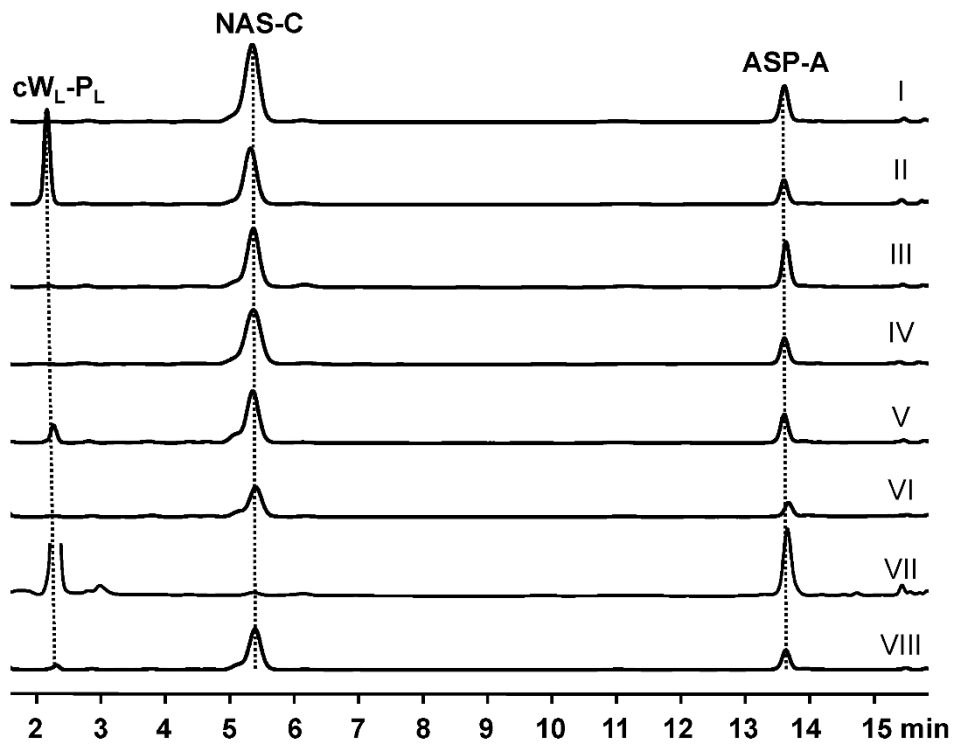
141

142



143

144 **Supplementary Fig. 5.** The eight fragments in the C-terminal part of $NascB$

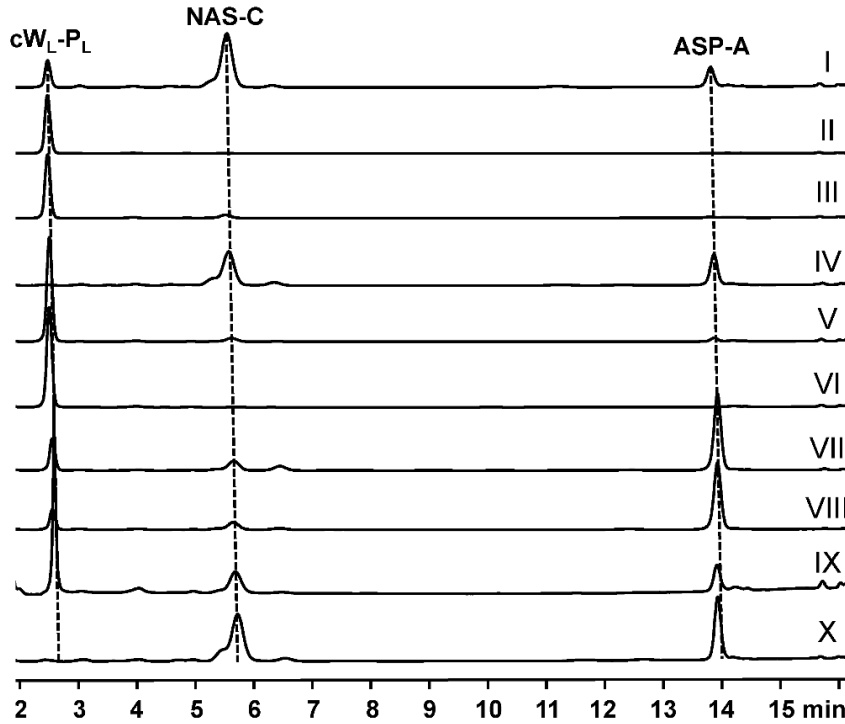


146

147

148 **Supplementary Fig. 6.** HPLC analysis of enzymatic conversion of cW_L-P_L by mutants
149 on the C-terminal part of NascB. I) NascB-S1868fragment-1; II) NascB-
150 S1868fragment-2; III) NascB-S1868fragment-3; IV) NascB-S1868fragment-4; V)
151 NascB-S1868fragment-5; VI) NascB-S1868fragment-6; VII) NascB-S1868fragment-7;
152 VIII) NascB-S1868fragment-8.

153

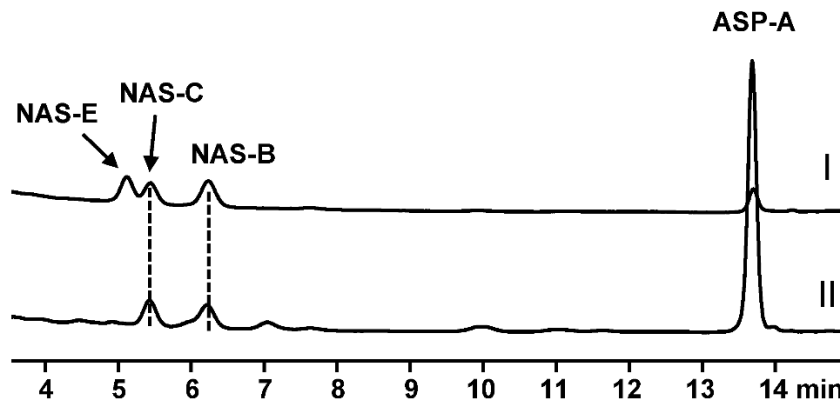


154

155

156 **Supplementary Fig.7.** HPLC analysis of enzymatic conversion of cW_L-P_L by mutants
 157 of NascB in fragment-7. I) NascB-Q65I-A86G-L298I; II) NascB-Q65I-A86G-H280Y; III)
 158 NascB-Q65I-A86G-A288V; IV) NascB-Q65I-A86G-A287S; V) NascB-Q65I-A86G-
 159 A284S; VI) NascB-S1868fragment-7-Y280H; VII) NascB-S1868fragment-7-S287A;
 160 VIII) NascB-S1868fragment-7-I298L; IX) NascB-S1868fragment-7-S284A; X) NascB-
 161 S1868fragment-7-V288A.

162



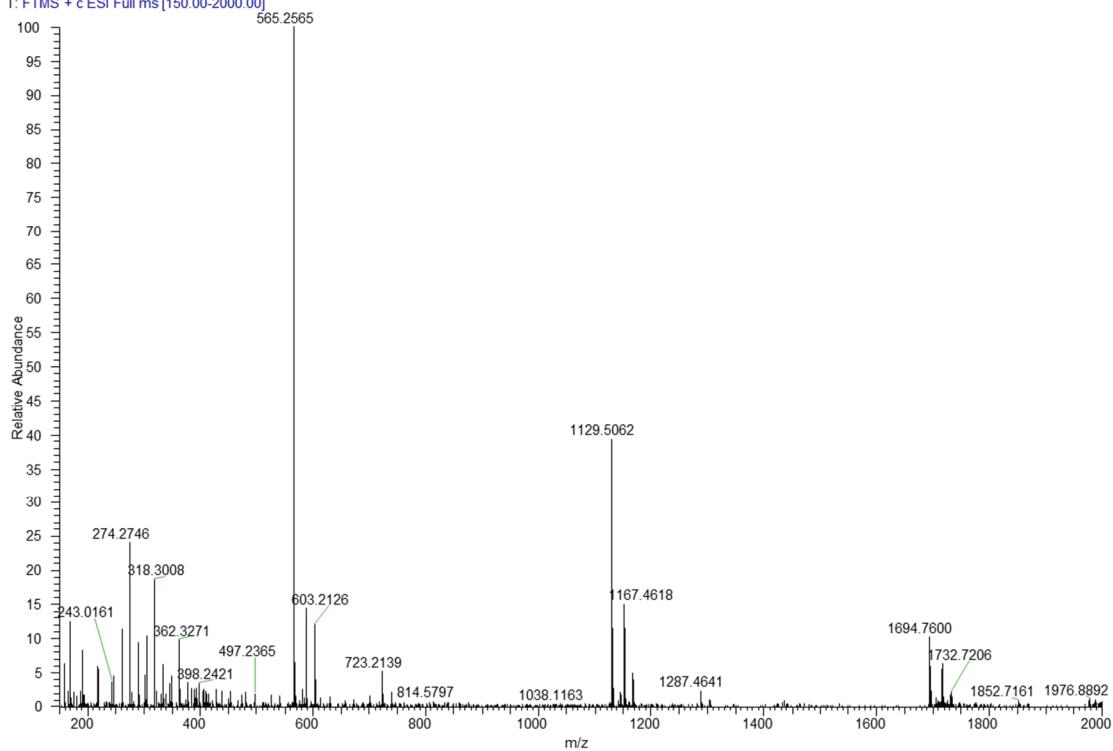
163

164

165 **Supplementary Fig. 8.** HPLC analysis of the Nas_{F5053} mutants which can improve the
 166 production of NAS-B. I) Nas_{F5053} -A89K; II) Nas_{F5053} -V288P.

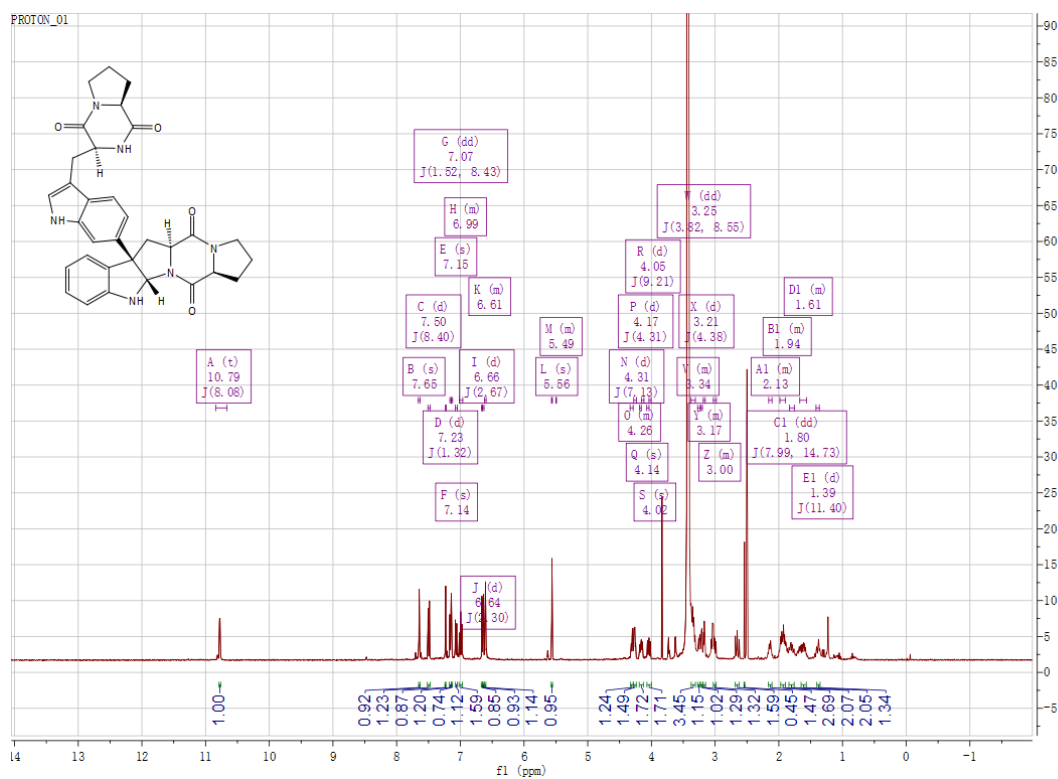
167 **a**

27-NEW#27 RT: 0.18 AV: 1 NL: 6.89E6
T: FTMS + c ESI Full ms [150.00-2000.00]



168

169 **b**

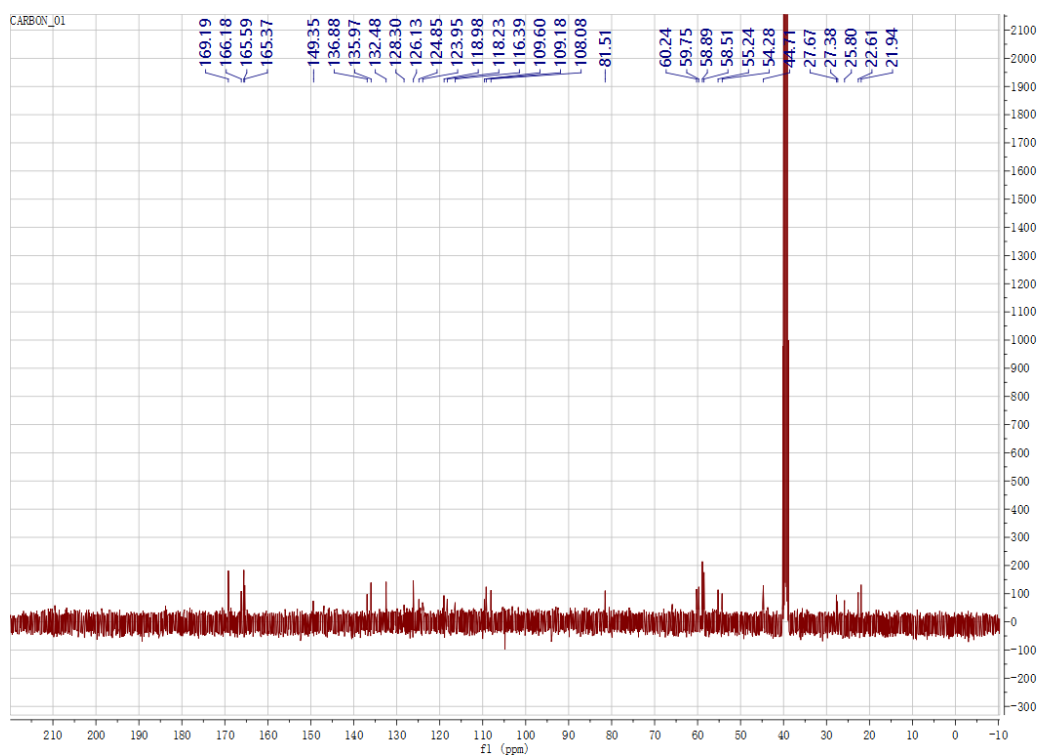


170

171

172

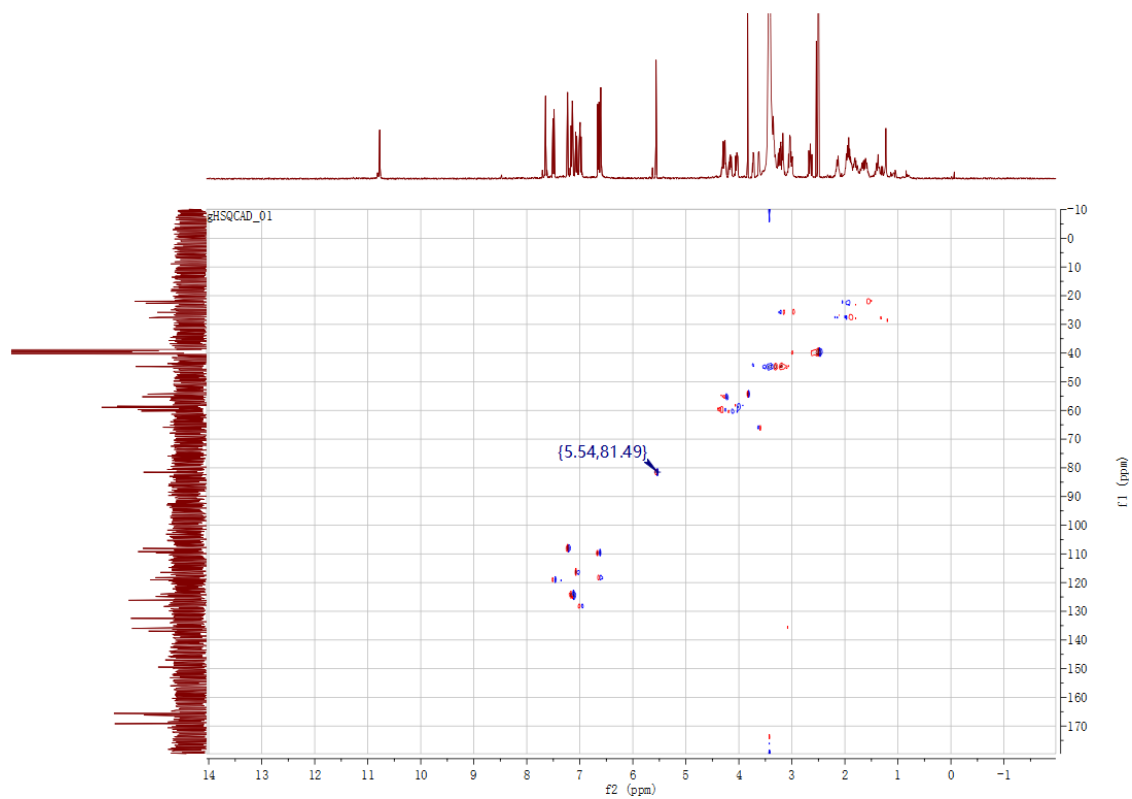
173 **c**



174

175

176 **d**

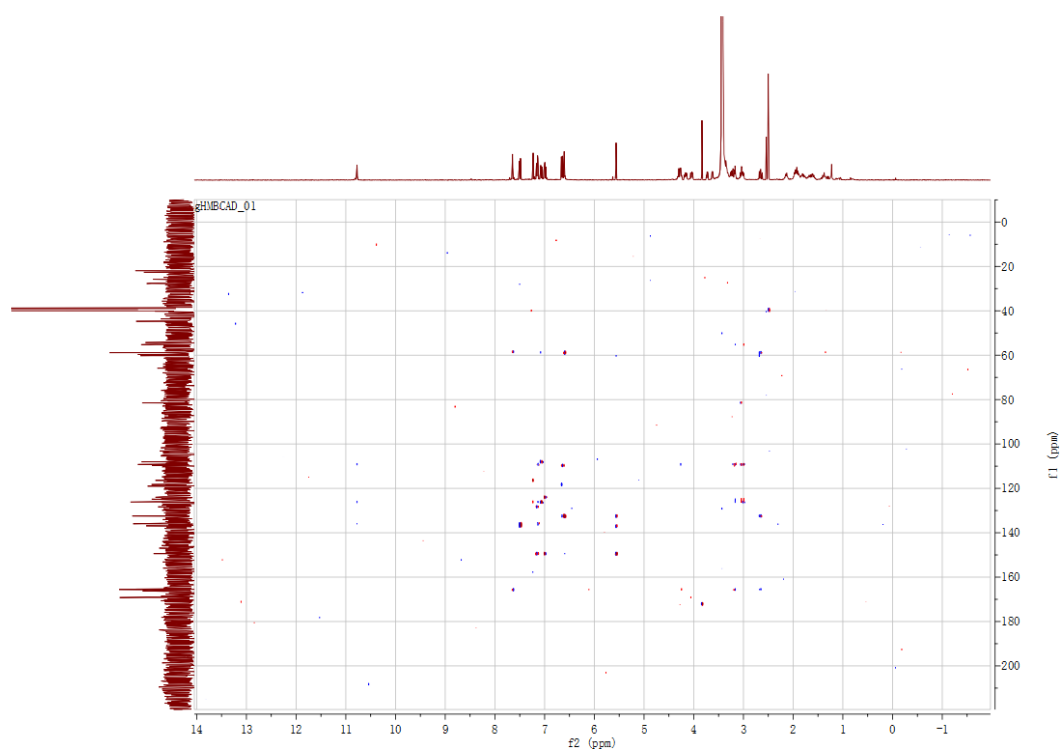


177

178

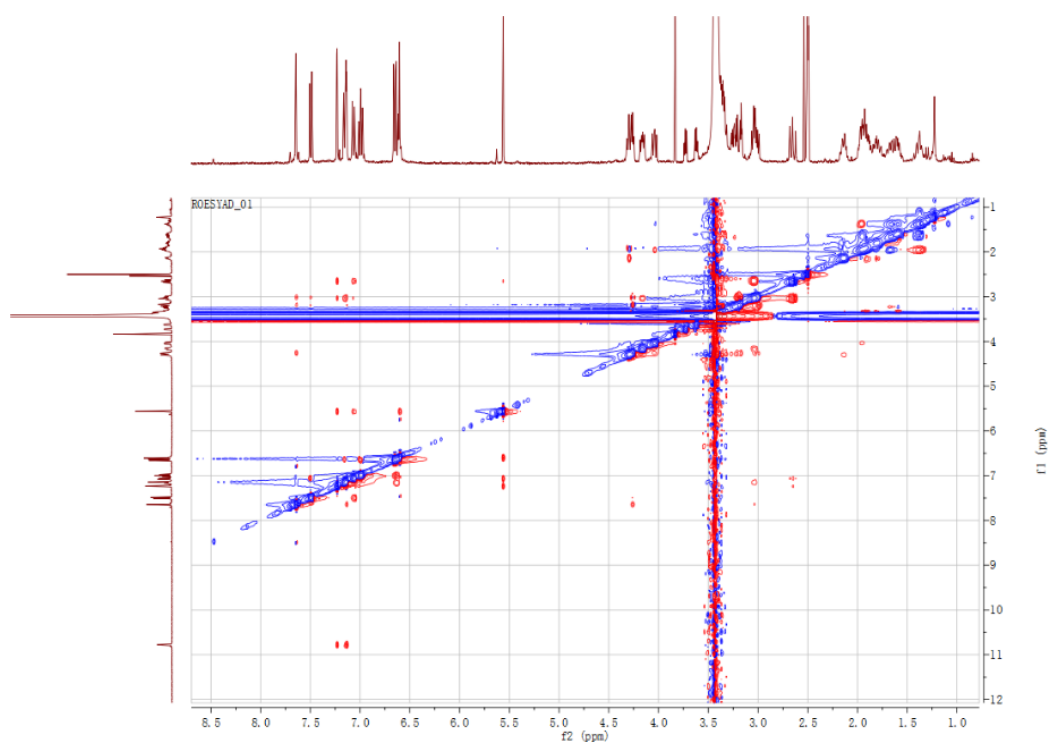
179

180 e



181

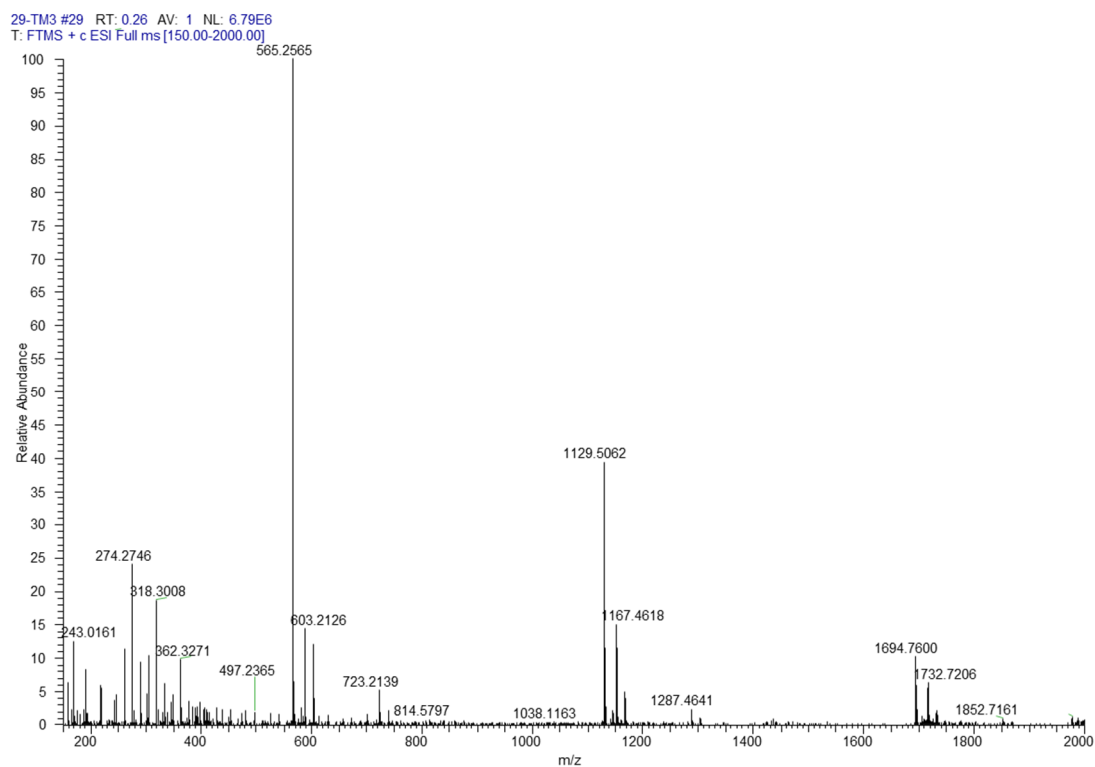
182 f



183

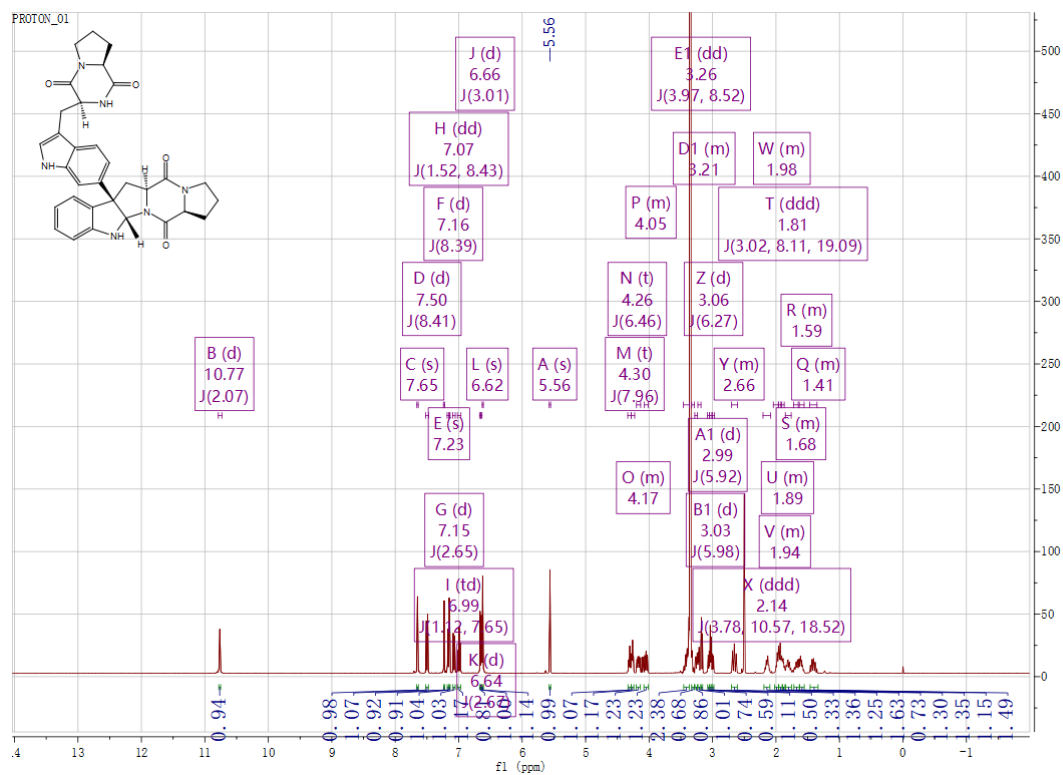
184 **Supplementary Fig. 9.** Spectra of compound NAS-E. (a) HRESIMS of compound of
185 NAS-E; (b) ^1H NMR of compound of NAS-E; (c) ^{13}C NMR of compound of NAS-E; (d)
186 HSQC of compound of NAS-E; (e) HMBC of compound of NAS-E; (f) ROSEY of
187 compound of NAS-E.

188 **a**



189

190 **b**

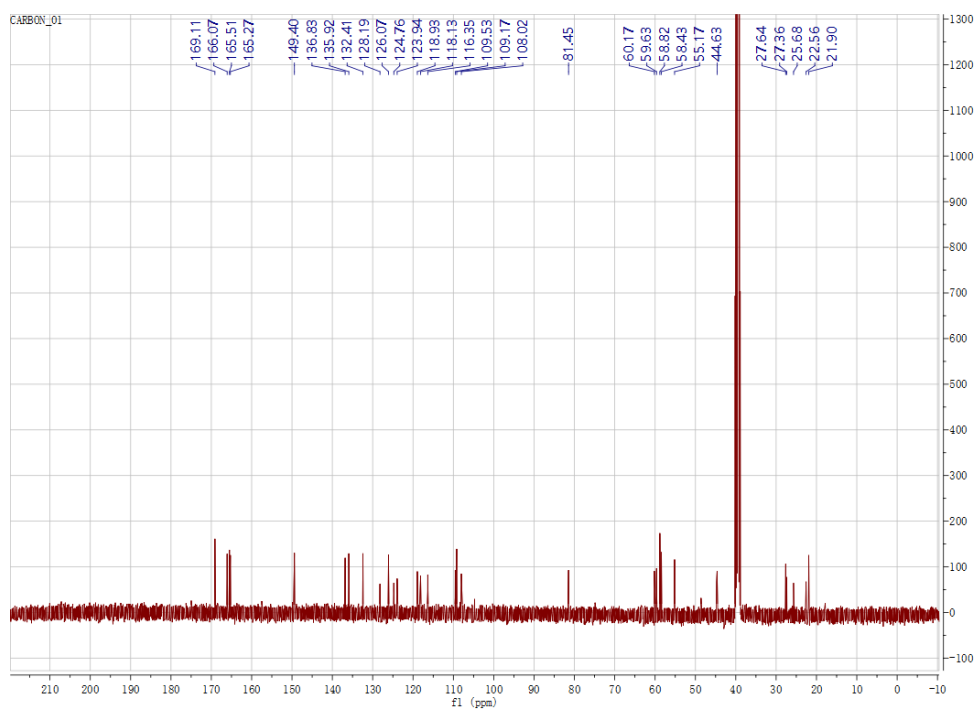


191

192

193

194 **c**

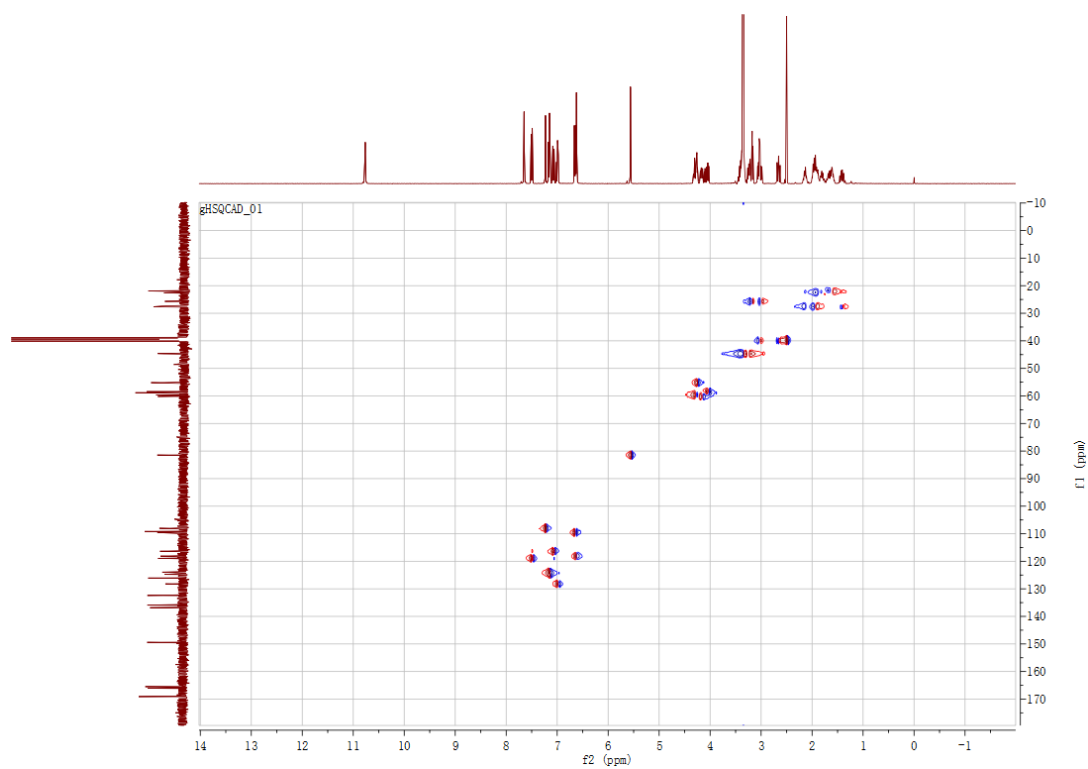


195

196

197

198 **d**

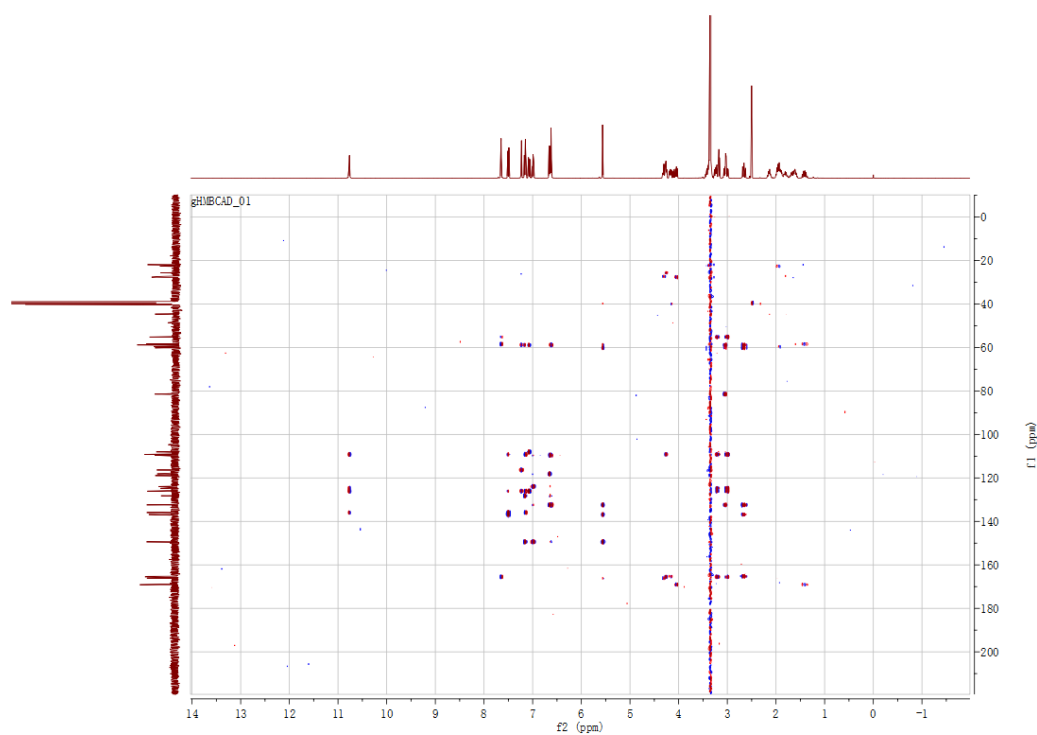


199

200

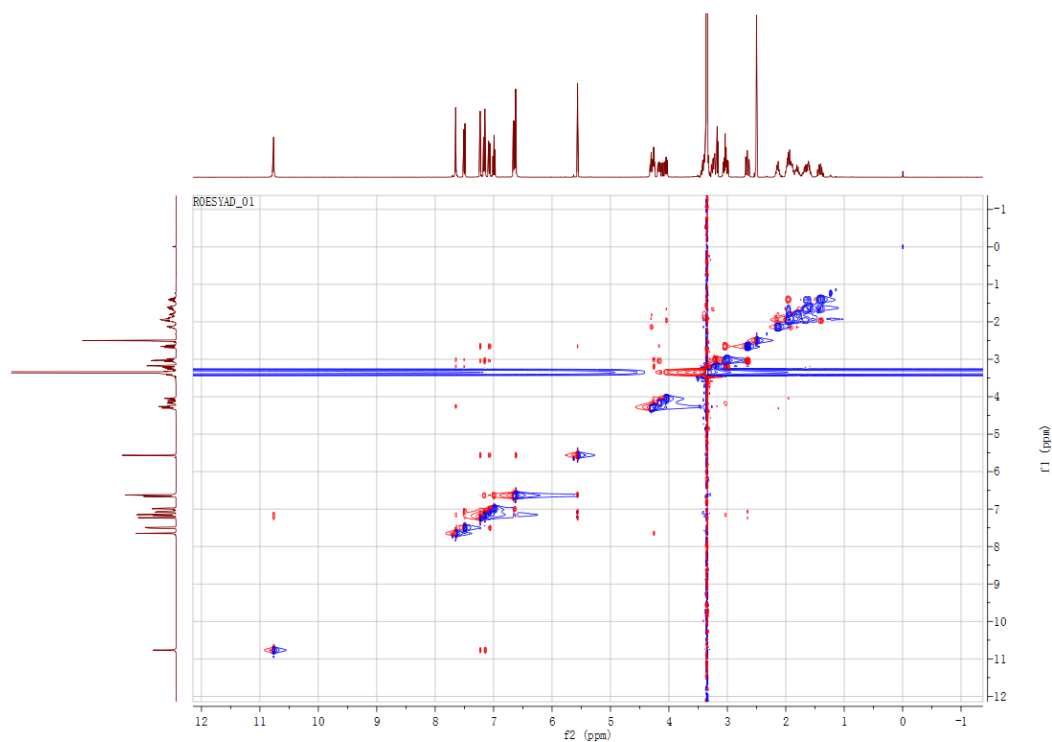
201

202 e



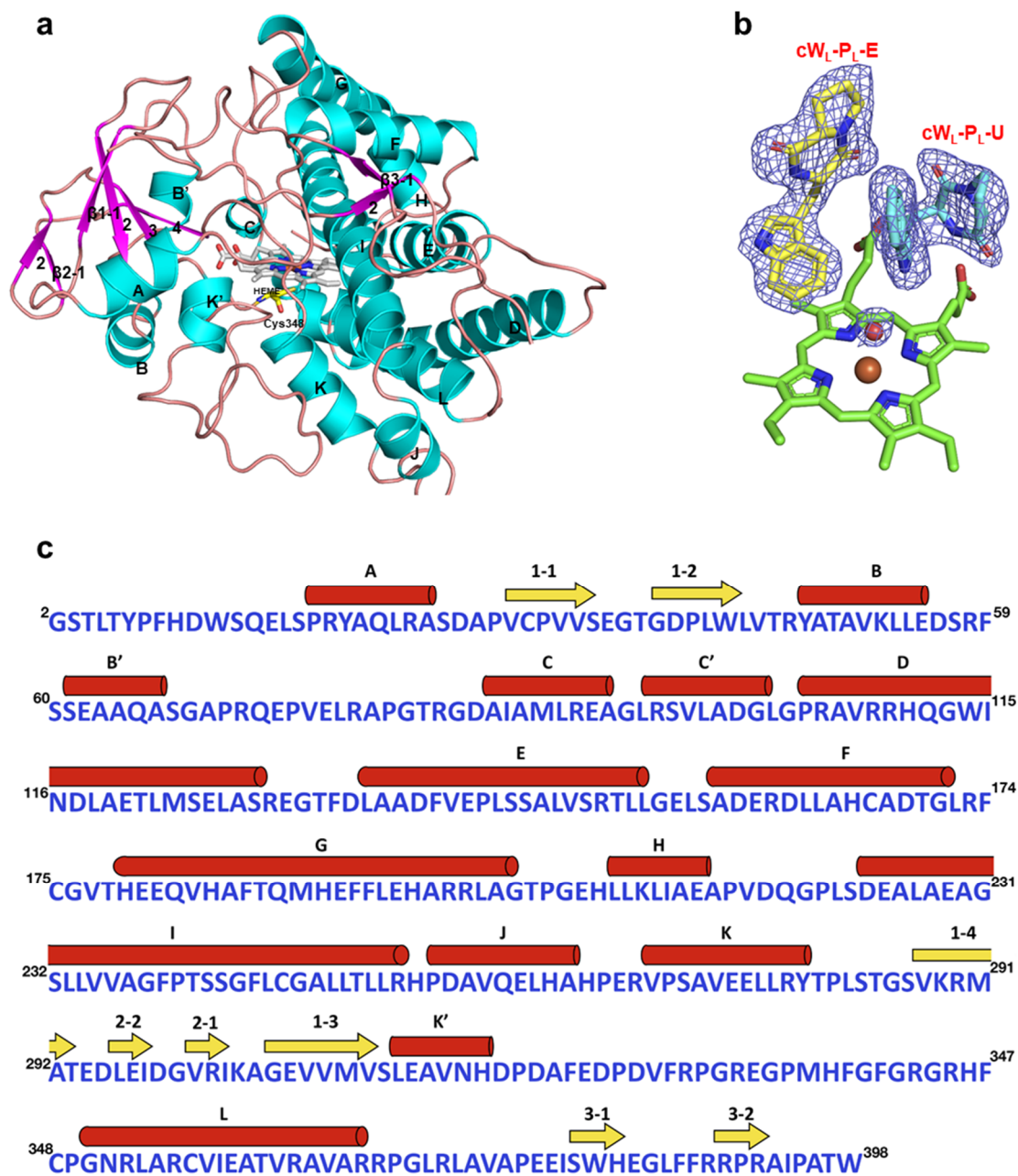
203

204 f



205

206 **Supplementary Fig. 10.** Spectra of the synthetic NAS-E (TM-3). (a) HRESIMS of
207 compound of TM-3; (b) ^1H NMR of compound of TM-3; (c) ^{13}C NMR of compound of
208 TM-3; (d) HSQC of compound of TM-3; (e) HMBC of compound of TM-3; (f) ROSEY
209 of compound of TM-3.



210

211

212 **Supplementary Fig. 11.** Crystal structure of Nas_{F5053}. (a) Cartoon representation of

213 the apo structure of Nas_{F5053}. The elements of secondary structure and the N- and C-

214 termini are labelled; α -helices are shown in cyan and β -strands in magenta. The iron

215 in the heme is shown as a brown sphere and water molecular is displayed as magenta

216 spheres. Other parts of the heme and cW_L-P_L-E/ U are displayed as green and yellow

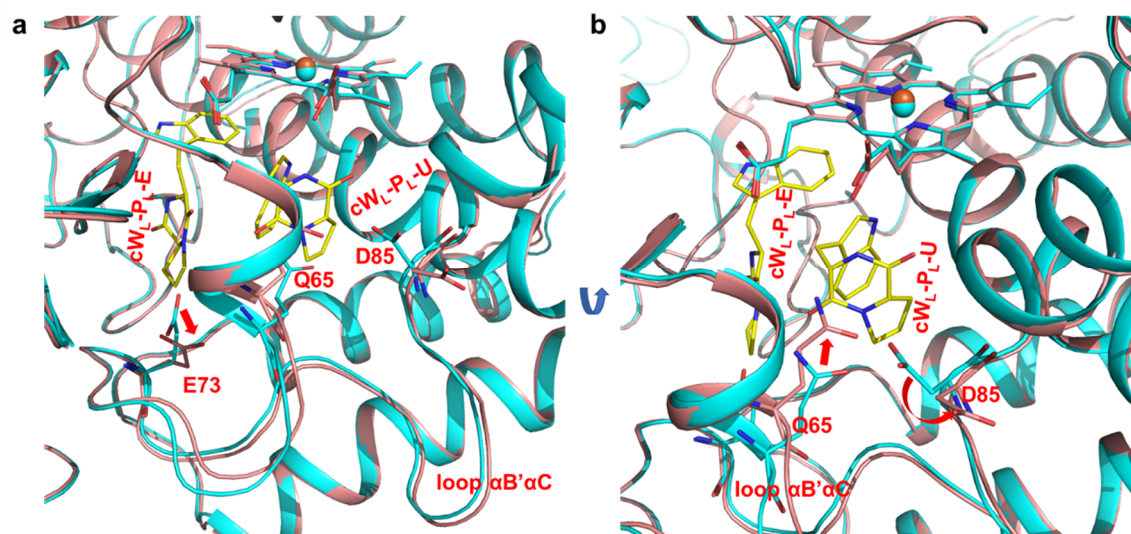
217 sticks, respectively. (b) Fo-Fc electron density omit map in the region of the cW_L-P_L-E

218 and cW_L-P_L-U substrates in the Nas_{F5053} complex structure (**Fig. 3a**), contoured at 4 σ

219 level (blue mesh). The map was calculated after 20 cycles of refinement in the absence
220 of the ligands. (c) The numbered amino-acid sequence of Nas_{F5053} used for structure
221 determination. Except for Gly2 and Ser3 added during the cloning process, the rest of
222 the sequence corresponds to the original Nas_{F5053} sequence. Labelled on the top of the
223 sequence is the elements of secondary structure, with yellow arrows for β -strands and
224 red cylinders for α -helices.

225

226



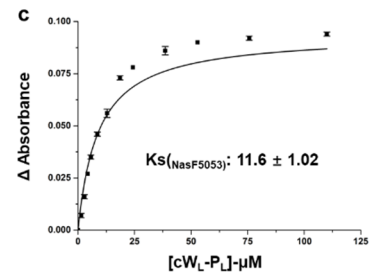
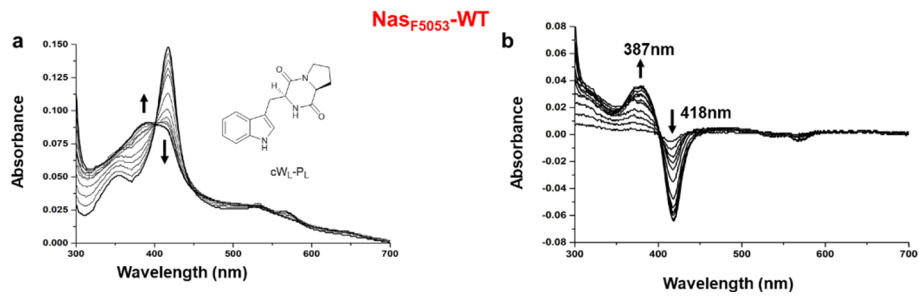
227

228

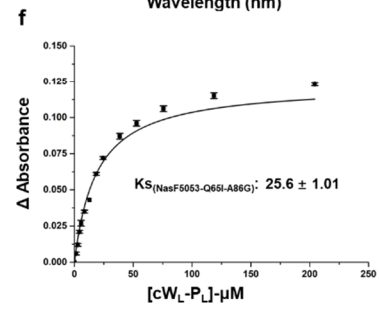
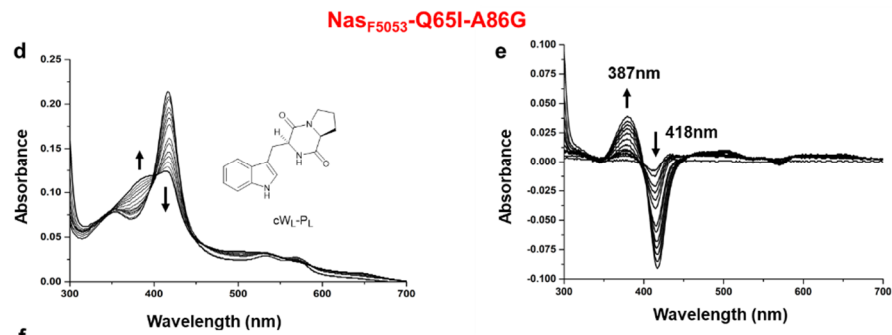
229 **Supplementary Fig. 12.** Superposition of Nas_{F5053} without the substrates (cyan) and
230 with the substrates (orange). (a) The two substrate molecules (cW_L-P_L-E and cW_L-P_L-
231 U) are colored yellow. Oxygen and nitrogen atoms are colored red and blue,
232 respectively. To accommodate substrates, the side-chains of D85 and E73 move away
233 from the binding site, while the side-chain of Q65 shifts towards cW_L-P_L-U. Those
234 movements are highlighted with red arrows. (b) As in Panel A, but rotated for a clearer
235 view of Q65. Q65, D82 and E73 are all located in the long loop α B'- α C.

236

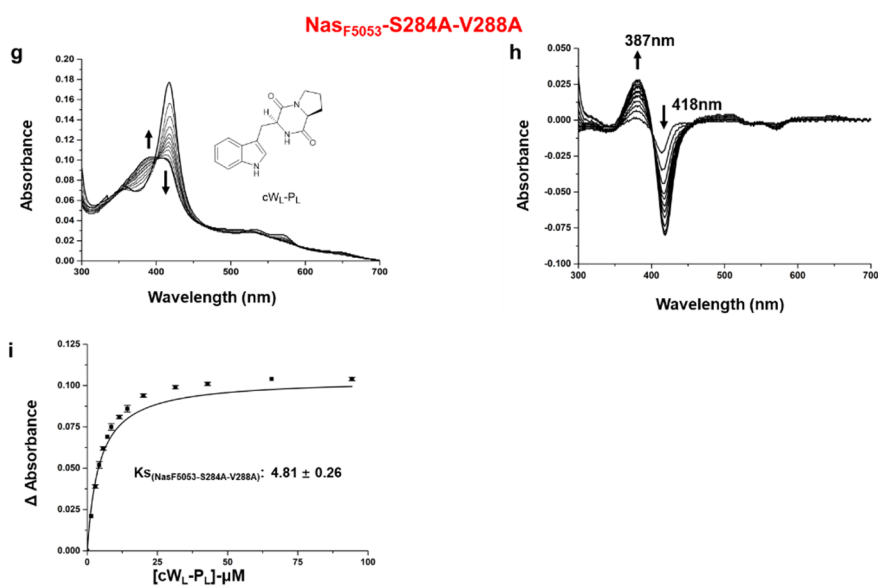
237



238
239
240



241



242

243 **Supplementary Fig. 13.** UV-Vis titration and determination of the binding constants of

244 cWL-PL to Nas_{F5053} (a-c), Nas_{F5053}-Q65I-A86G (d-f) and Nas_{F5053}-S284A-V288A (g-i).

245 The chemical structure of cWL-PL is included beside UV absorption curve. Arrows

246 indicate directions of change in spectra upon addition of cWL-PL. All these experiments

247 are conducted independently in triplicate (n=3). The averaged values from triplicate

248 were used to make plots. (a) Spectral titration of 2 μ M Nas_{F5053} with 0–110 μ M cWL-PL.

249 Spectra corresponding to 0 and 110 μ M cWL-PL are highlighted in bold black. (b)

250 Difference spectra. (c) The fitting of titration points to a rectangular hyperbola curve for

251 calculating the binding constant. (d) Spectral titration of 2 μ M Nas_{F5053}-Q65I-A86G with

252 0–204 μ M cWL-PL. Spectra corresponding to 0 and 204 μ M cWL-PL are highlighted in

253 bold black. (e) Difference spectra for Nas_{F5053}-Q65I-A86G. (f) The fitting of titration

254 points to a rectangular hyperbola curve for calculating the binding constant. (g).

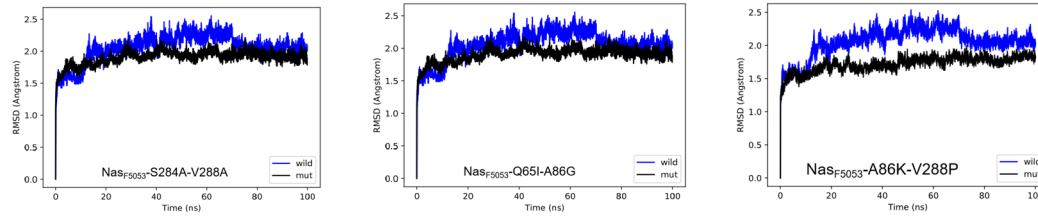
255 Spectral titration of 2 μ M Nas_{F5053}-S284A-V288A with 0–95 μ M cWL-PL. Spectra

256 corresponding to 0 and 95 μ M cWL-PL are highlighted in bold black. (h) Difference

257 spectra (i) The fitting of titration points to a rectangular hyperbola curve for calculating

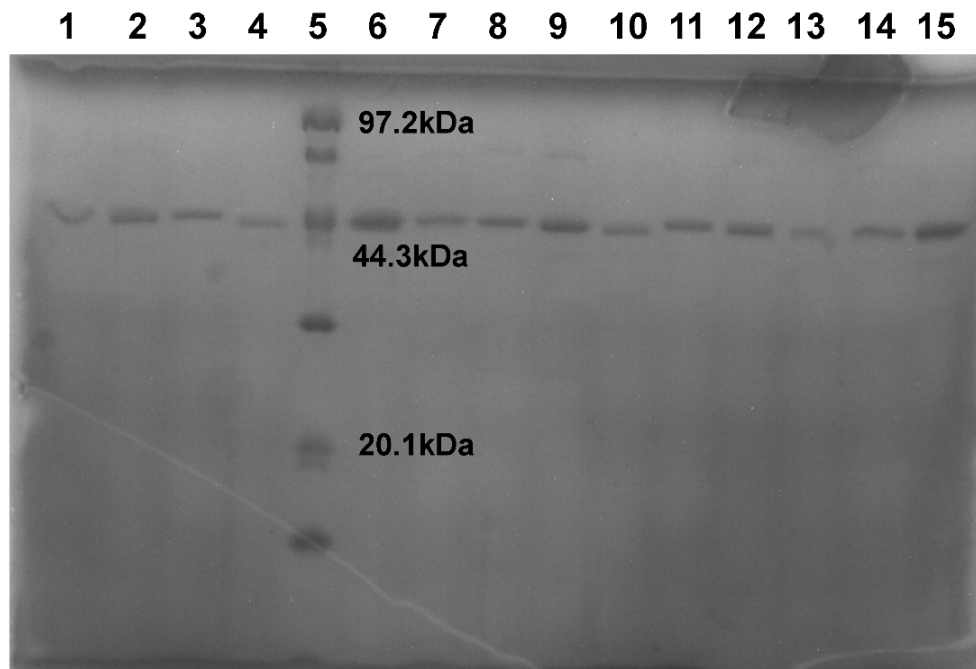
258 the binding constant.

259



260
261
262
263
264

Supplementary Fig. 14. RMSD variation in molecular dynamics simulations.



265
266
267
268
269
270
271
272
273
274
275

Supplementary Fig. 15. SDS-PAGE analysis of recombinant proteins. Lane 1: Nas_{S1868}, 44kDa; Lane 2: Nas_{F5053}, 44 kDa; Lane 3: Nas_{bB}, 44 kDa; Lane 4: Nas_{F5053-Q65I}, 44 kDa; Lane 5: Marker; Lane 6: Nas_{F5053-A86G}, 44 kDa; Lane 7: Nas_{F5053-A86G-Q65I}, 44 kDa; Lane 8: Nas_{F5053-S284A}, 44 kDa; Lane 9: Nas_{F5053-V288A}, 44 kDa; Lane 10: Nas_{cB-Q65I}, 44 kDa; Lane 11: Nas_{cB-A86G}, 44 kDa; Lane 12: Nas_{cB-Q65I-A86G}, 44 kDa; Lane 13: Nas_{cB-S1868fragment-7}, 44 kDa; Lane 14: Nas_{cB-Q65I-A86G-A284S-A288V}, 44 kDa; Lane 15: Nas_{F5053-A86K-V288P}, 44 kDa.

276 **2. Supplementary Tables**

277

278 **Supplementary Table 1.** Product profiles and yields of the P450 reactions using cW_L-279 P_L as substrate (NasB, NasbB, NascB, Nas_{F5053} and AspB).

280

Products & yields P450s	NAS-B	NAS-C	ASP-A	Iso-NAS-B
NasB ^a	93.5%	0	6.5%	0
NasbB	100%	0	0	0
NascB	0	100%	0	0
Nas _{F5053}	8.2%	47.4%	44.4%	0
Nas _{S1868}	0	0	100%	0
AspB ^a	0%	1.5%	98.1%	0.4%

281 ^adata were achieved from Li's paper¹.

282

283 **Supplementary Table 2.** NMR data of compound NAS-B in DMSO-*d*₆.

284

no.	δ_H	δ_C	¹H-¹³C HMBC	ROESY
2	5.65, d,(3.2)	85.0	7'	11,1-NH,12b,8'
3		59.9		
4		134.7		
5	6.73,d,(3.2)	123.5	3,7,9	
6	6.54,m	118.2	8	
7	6.97,m	128.1	5, 9	
8	6.57,m	109.4	4,6	
9		148.2		
11	4.66,m	59.6	12,13	2,12a
12a	3.10,m	38.8	2,3,7'	
12b	2.33,m		3,13,7'	
13		166.1		
15	4.30,s	60.1	16,17	

16		168.1	
17a	2.11,m	27.2	
17b	1.35,m		
18a/b	1.80,m,(2H)	23.1	
19a/b	3.21,m,(2H)	44.7	
2'	7.15,s	125.2	3',4',9'
3'		109.2	
4'		126.2	
5'	7.53,d,(8.4)	119.3	3',7'
6'	6.93,m	118.0	3,4',8'
7'		135.7	
8'	7.28,s	109.3	3,4',6'
9'		136.0	
11'	4.25,m	55.3	3',12',13'
12'a	3.16,m	25.9	
12'b	3.02,dd,(14.5,4.5)		2',3',11',13'
13'		165.6	
15'	4.02,m	58.6	16',17'
16'		169.3	
17'a/b	1.93,m,(2H)	27.8	
18'a/b	1.60,m,(2H)	22.0	
19'a/b	3.33,m,(2H)	44.7	
1-NH	6.69,s		3,4,9
1'-NH	10.85,s		3',4',9'
10'-NH	7.63,s		11',15',16'

285

286

287

288

289

290

291

292

293

294

295 **Supplementary Table 3.** NMR data of compound ASP-A in DMSO-*d*₆.

<i>no.</i>	$\delta_{\text{H,mult}}$ (<i>J</i> in Hz)	δ_{C}	$^1\text{H-}^{13}\text{C}$ HMBC
2	7.28,d,(2.3)	125.7	3,4,9
3		109.7	
4		126.1	
5	7.74,d,(8.4)	119.7	3,7,9
6	7.14,dd,(8.7,1.4)	115.2	4,8
7		133.1	
8	7.44,d,(1.7)	106.7	4,6
9		136.1	
11	4.36,m	55.3	3,12,13
12a	3.31,m	25.8	11
12b	3.29,m		
13		165.5	
15	4.10,m	58.5	16,17
16		169.1	
17a/b	1.40,m(2H)	27.7	
18a/b	1.70,m(2H)	21.9	
19a	3.28,m	44.6	
19b	3.26,m		
2'	7.46,s	128.3	3',4',9',7'
3'		111.0	
4'		128.3	
5'	7.68,d,(7.8)	119.4	3',7',9'
6'	7.47,d,(8.2)	110.1	4',8'
7'	7.17,m	122.0	5',9'
8'	7.10,m	119.4	4',6'
9'		135.6	
11'	4.40,m	55.2	3',12',13'

12'a	3.16,d,(5.6)	25.9	2',3',4',11',13'
12'b	3.13,d,(5.6)		2',3',4',11',13'
13'		165.4	
15'	4.08,m	58.5	16',17'
16'		169.0	
17'	2.00,m,(2H)	27.7	
18'	1.61,m,(2H)	21.8	
19'a	3.42,m	44.6	
19'b	3.38,m		
1-NH	11.05,d,(2.2)		3,4,9
10-NH	7.85,s		11,15,16
10'-NH	7.97,s		11',15',16'

297

298

299

300

Supplementary Table 4. NMR data of compound NAS-E in DMSO-*d*₆.

<i>no.</i>	δ_{H}	δ_{C}	$^1\text{H}-^{13}\text{C}$ HMBC	ROESY
2	5.56,s	81.4	4,9,7'	1-NH,6',8'
3		58.8		
4		132.4		
5	7.16,d,(8.4)	124.0	3,7,9	
6	6.66,m	109.5	8	
7	6.99,dd,(7.6,1.1)	128.2	5,9	
8	6.64,d,(2.6)	118.1	4,6	
9		149.4		
11	4.17,m	60.2	13	
12a	3.06,m	40.0	2,4	
12b	2.66,m		3,4,13,7'	
13		165.3		
15	4.30,s	59.6	17,18	
16		166.1		

17a	2.14,m	27.4	
17b	1.98,m		
18a	1.94,m	22.6	
18b	1.81,m		
19a	3.17,m	44.6	
19b	3.26,m		
2'	7.14,d,(2.6)	124.8	3',4',9'
3'		109.2	
4'		126.1	
5'	7.50,d,(8.4)	119.0	3',9'
6'	7.07,dd,(8.4,1.5)	116.4	4',8',3,
7'		136.8	
8'	7.23,s	108.0	3,4',6'
9'		136.0	
11'	4.26,m	55.2	3',12',13'
12'a	3.22,m	25.7	2',3',4',11',13'
12'b	3.03,m		
13'		165.5	
15'	4.05,m	58.4	16',17'
16'		169.1	
17'a	1.89,m	27.6	
17'b	1.41,m		15',16'
1-NH	6.62,s		3,4
1'-NH	10.77,d,(2.1)		3',4',9'
10'-NH	7.65,s		13',15'

301

302

303

304

305 **Supplementary Table 5.** X-ray data collection and structure refinement statistics for

306 Nas_{F5053} and its mutants.

307

	Substrate-bound Nas _{F5053}	Ligand-free Nas _{F5053}	Substrate-bound Nas _{F5053} - Q65I/A86G	Substrate-bound Nas _{F5053} - S84A/V288A
Data collection				
Space group	P 2 2 ₁ 2 ₁	P 2 ₁	P 2 2 ₁ 2 ₁	P 2 2 ₁ 2 ₁
Cell dimensions				
<i>a</i> , <i>b</i> , <i>c</i> (Å)	42.31, 91.84, 93.60	42.21, 91.33, 98.26	42.23, 91.31, 93.81	42.24, 91.21, 93.46
α , β , γ (°)	90.00, 90.00, 90.00	90.00, 96.41, 90.00	90.00, 90.00, 90.00	90.00, 90.00, 90.00
Wavelength (Å)	0.954	0.954	0.954	0.954
Resolution (Å)	46.80-1.60 (1.63-1.60)	43.06-1.70 (1.76- 1.70)	38.51-1.47 (1.52- 1.47)	46.73-1.68 (1.74- 1.68)
CC1/2	0.99 (0.71)	1.00 (0.79)	1.00 (0.68)	1.00 (0.74)
<i>R</i> _{merge}	0.085 (1.177)	0.035 (0.326)	0.026 (0.329)	0.039 (0.335)
Average <i>I</i> / σ (<i>I</i>)	11.8 (1.7)	9.1 (2.2)	14.7 (2.2)	12.5 (2.1)
Completeness (%)	99.9 (99.7)	99.7 (99.1)	98.4 (95.6)	98.1 (96.4)
Multiplicity	6.7	6.4	6.8	6.7
Refinement				
Resolution (Å)	46.80-1.60 (1.63-1.60)	43.06-1.70 (1.76- 1.70)	38.51-1.47 (1.52- 1.47)	46.73-1.68 (1.74- 1.68)
No. unique reflections	48951 (2415)	81166 (8040)	61852 (5917)	41354 (3988)
<i>R</i> _{work} / <i>R</i> _{free} (%)	16.9/20.3	19.3/21.9	15.5/18.0	16.9/24.7
No. atoms				
Protein	3068	6133	3050	3037

Ligand/ion	5	13	8	2
Water	351	812	423	342
<i>B</i> -factors (Å ²)				
Protein	25.9	23.1	18.9	19.0
Ligand/ion	18.3	16.5	14.7	12.5
Water	35.9	32.5	30.1	26.0
R.m.s deviations				
Bond lengths	0.005	0.023	0.009	0.010
(Å)				
Bond angles (°)	0.81	1.79	1.09	1.11

308 *Values in parentheses are for the highest-resolution shell.

$$R_{\text{merge}} = \frac{\sum_{hkl} \sum_j |I_{hkl,j} - \langle I_{hkl} \rangle|}{(\sum_{hkl} \sum_j I_{hkl,j})}$$

$R_{\text{work}} / R_{\text{free}} = \frac{\sum_{hkl} |F_{hkl}^{\text{obs}} - F_{hkl}^{\text{calc}}|}{(\sum_{hkl} F_{hkl}^{\text{obs}})}$; R_{free} was calculated using randomly chosen 5-10 % fraction of data that was excluded from refinement.

309 **Supplementary Table 6.** Bacterial strains and plasmids.

310

Strains	Description	Source
DH5α	Host for general cloning	Invitrogen
BL21 (DE3)	Host for protein expression	Invitrogen
GB05-dir-T7	Host for protein expression	This study
<i>M. smegmatis</i> mc ² 155	Host for protein expression	From Prof. Jiaoyu Deng
Plasmids		
pET28a	Protein expression vector in <i>E. coli</i>	Novagen
pET21a	Protein expression vector in <i>E. coli</i>	Novagen
pMF406	Protein expression vector in <i>M. smegmatis</i> mc ² 155	From Prof. Xiaoyong Fan ²

pMV261	Protein expression vector in <i>M. smegmatis</i> mc ² 155	From Prof Jiaoyu Deng
pMV261-ACE	pMV261 derivative containing pACE	This study
pSrtA9		6
pMS1	Protein expression vector in <i>M. smegmatis</i> mc ² 155	This study
pSJTU1	pET28a derivative for Nas _{F5053} expression in <i>E. coli</i>	This study
pSJTU2	pMS1 derivative for NasbB expression in <i>M. smegmatis</i> mc ² 155	This study
pSJTU3	pMS1 derivative for Nas _{S1868} expression in <i>M. smegmatis</i> mc ² 155	This study
pSJTU4	pET21a derivative, containing Nas _{F5053} gene	This study
pWHU2487	pRSF-Duet derivative for Trx-Fd and MBP-FdR co-expression in <i>E. coli</i>	3
pWHU2485	pET28a derivative for NascB expression in <i>E. coli</i>	3

311

312

313 **Supplementary Table 7.** Primers used in this study.

314

Name	Sequence (5' to 3')
F5053-F	tggtgccgcgcgccagccatgATGACCACCACCGCAACCCTGACC
F5053-R	ttgtcgacggagctcgaattcTTACCATGTTGCCGGAATGGCGCGC
F5053-overlap-R	GCTGCGGCGTAGCGTGTTGCCAGCCACAGATGGTCAC
F5053-overlap-F	ACACGCTACGCCGAGCCGTGGAAGTCTGGAAG
F5053-A86G-F	CGGTGACGGTATTGCAATG
F5053-A86G-R	CATTGCAATACCGTCACCG

F5053-Q65I-F	GAAGCCGCAATTGCCAGTGGT
F5053-Q65I-R	ACCACTGGCAATTGCGGCTTC
F5053-I87V-F	GGTGACGCCGTGGCAATGCTG
F5053-I87V-R	CAGCATTGCCACGGCGTCACC
F5053-G84A-F	GTACACGCGCCGACGCCATTG
F5053-G84A-R	CAATGGCGTCGGCGCGTGTAC
F5053-Xray-For	GCCGGAACCGGCTCTACCCTGACCTACCCGTTTCATGAC
F5053-Xray-Rev	GCAAAGCACCGGGGCTTACCATGTTGCCGGAATGGCG
Nas _{F5053} -S284A- V288A-For	cagcgcaAAACGCATGGCCACCGAA
Nas _{F5053} -S284A- V288A-Rev	cctgttgcCAGAGGGGTATAACGCAGC
nascB-A86G-F	TACACGTGGTGACGGTATCGCAATG
nascB-A86G-R	GTAACATTGCGATACCGTCACCACG
nascB-Q65I-F	TGAAGCCGCAATTGCAAGCGGTGC
nascB-Q65I-F	CGGGGCACCGCTTGCAATTGCG
nascB-P40H-F	TACCGGCGATCATCTGTGGCTGG
nascB-P40H-R	TAACCAGCCACAGATGATCGCCG
nascB-V44A-F	CTGTGGCTGGCAACCCGCTATGC
nascB-V44A-R	GTGGCATAGCGGGTTGCCAGCCA
nascB-T49A-F	ACCCGCTATGCCGCCGCCGTTAA
nascB-T49A-R	AGTTTAACGGCGGCGGCATAGCG
nascB-K52E-F	CACCGCCGTTGAACTGCTGGAAG
nascB-K52E-R	TGTCTTCCAGCAGTTCAACGGCGGT
nascB-S57F-F	GCTGGAAGACTTCCGCTTCAGCA
nascB-S57F-R	CACTGCTGAAGCGGAAGTCTTCC
nascB-G84A-F	GGTACACGTGCAGACGCAATCGC
nascB-G84A-R	ATTGCGATTGCGTCTGCACGTGT
nascB-I87V-F	GGTGACGCAGTGGCAATGTTA

nascB-I87V-R GTAACATTGCCACTGCGTCAC
nascB-For tggtgccgcgcgccagccatgATGACCACCACCGCAACCCTG
nascB-Rev ttgtcgacggagctcgaattcCCAGGTGGCAGGCAGTGCGC
nascB-fragment1-R GCTCATCAGGGTTTCGGCCAGATCATTAAATCCAGCCC
nascB- fragment1-F GCCGAAACCCTGATGAGCGCACTGGCCAGCCGTGAAG
nascB- fragment2-R CTGCTCAGAGGTTCCACAAAATCGGCTG
nascB- fragment2-F GATCTGGCAGCCGATTTTGTGGAACCTC
nascB- fragment3-R GCGCAGGCCTGTGTCTGCACAGTGTGCCAGCAGATCGC
nascB-fragment3-F GCAGACACAGGCCTGCGCTTTTTCGGCGTGACCCATG
nascB-fragment4-R GCTCCAGAAAAAATTCGTGCATCTGGGTGAAGGCGTGAACC
nascB-fragment4-F ACGAATTTTTTCTGGAGCATGCACGTCGCTTAGCAGGCACCCC
nascB-fragment5-R CATCGCTTAACGGACCATGATCCACCGGTGCCTCGGCAATCAGT
T
nascB-fragment5-F ATGGTCCGTTAAGCGATGAAGCCCTGGCCGAAGCAGGCAGCCT
GC
nascB-fragment6-R CAGCTCCTGCACGGCATCCGGGTGACGCAGCAGTGTGAGCA
nascB-fragment6-F CACCCGGATGCCGTGCAGGAGCTGCATGCACATCCGGAACGCG
T
nascB-fragment7-R CATGCGTTTCACGCTGCCTGTGCTCAGCGGTGTATAGCGC
nascB-fragment7-F GGCAGCGTGAAACGCATGGCAACAGAGGACCTGGAGATTGA
nascB-fragment8-R CCTCCAGGCTAACCATCACACCTCACCCACTTTAAT
nascB-fragment8-F GTGATGGTTAGCCTGGAGGCCGTTAACCATGACCCGG
nascB-H280Y-F ACTGCTGCGCTATACACCGCTGGCA
nascB-H280Y-R TGCCAGCGGTGTATAGCGCAGCAGT
nascB-A288V-F ACAGGCGCCGTGAAACGCATGGCA
nascB-A288V-R TGCCATGCGTTTTACGGCGCCTGT
nascB-A287S-F CTGGCAACAGGCAGCGCAAAACGCA
nascB-A287S-R TGCGTTTTGCGCTGCCTGTTGCCAG
nascB-A284S-F CATACACCGCTGAGCACAGGCGCCG

nascB-A284S-R	CGGCGCCTGTGCTCAGCGGTGTATG
nascB-Y280H-F	GAAGTGTGCGCCATACACCGCTG
nascB-Y280H-R	GCTCAGCGGTGTATGGCGCAGCAG
nascB-V288A-F	CACAGGCAGCGCAAACGCATGG
nascB-V288A-R	TGCCATGCGTTTTGCGCTGCCTG
nascB-S287A-F	GAGCACAGGCGCCGTGAAACGCAT
nascB-S287A-R	CCATGCGTTTTACGGCGCCTGTGC
nascB-S284A-F	TACACCGCTGGCAACAGGCAGCG
nascB-S284A-R	CACGCTGCCTGTTGCCAGCGGTG
nascB-I298L-F	GGACCTGGAGCTGGATGGTGTTT
nascB-I298L-R	ACGAACACCATCCAGCTCCAGGT
Nas _{F5053} -S284A-F	ATACCCCTCTGGCAACAGGCAGC
Nas _{F5053} -S284A-R	TCACGCTGCCTGTTGCCAGAGGGT
Nas _{F5053} -V288A-F	GCACAGGCAGCGCAAACGCATG
Nas _{F5053} -V288A-R	GGCCATGCGTTTTGCGCTGCCTGT
Nas _{F5053} -SM-NNK-F	CGCANNKGCCAGTGGTGCACCGCGTCAGGAACCGGTGGAATTA CGTGCCCCGGGTACACGCGGTGACNNKAT
Nas _{F5053} -SM-NNK-R	TGGCCATGCGTTTMNNGCTGCCTGTMNNCAGAGGGGTATAACG CAG
Ami-for	TTTTCTAGAGAAGTGACGCGGTCTCAAGCG
Ami-rev	TTTGGATCCGAAAACCTACCTCGGGCATGTGGAC
tev-for	GATCGCACCATCACCATCACCACGGTGGTTCGGGCGAGAACCT GTACTTCCAGGGATCCCATATGG
tev-rev	CGTGGTAGTGGTAGTGGTGCCACCAAGCCCGCTCTTGGACATG AAGGTCCCTAGGGTATACCTTAA

316 **3. Supplementary Methods**

317 **3.1. General materials and methods**

318 *Escherichia coli* and *Mycobacterium* strains were cultivated and manipulated
319 according to standard methods^{2,4}. *Mycobacterium smegmatis* mc² 155 was cultivated
320 either on Luria-Bertani (LB) media agar plates or in Lemoco liquid media (5 g peptone,
321 5 g beef extract, 5 g NaCl, 0.1 % Tween 80 in 1 L tap water). Strains and plasmids
322 used in this study are listed in **Supplementary Table 6**. Primer synthesis and DNA
323 sequencing were performed at Genewiz Biotech Co., Ltd. (China). All the primers used
324 in this study are all listed in **Supplementary Table 7**. Restriction enzymes and DNA
325 polymerases (Taq and PrimeSTAR) were purchased from Takara Biotechnology Co.,
326 Ltd. (China). Discovery Studio was used to analysis the interactions between ligands
327 and the enzymes. All chemicals and reagents were purchased from Santa Cruz
328 Biotechnology, Inc. (USA) or Shanghai Sangon Biotech (China) Co., Ltd., unless noted
329 otherwise, and all the chemical structures were drawn with ChemBioDraw. HPLC
330 analysis was carried out on an SHIMADZU LC-30A UPLC system. UPLC-MS analysis
331 was carried out on a SHIMADZU LC-30A system connected to a single quadrupole
332 mass spectrometer MS2020 (ESI). ESI-high resolution MS (ESI-HRMS) analysis was
333 carried out on ESI-LTQ Orbitrap (ThermoFisher Scientific Inc.). NMR analysis was
334 carried out on a Bruker DRX-400 NMR spectrometer (Bruker Co. Ltd., Germany).

335

336 **3.2. Cloning, expression and purification of P450s and associated proteins**

337 The DNA sequences of Nas_{F5053}, NasbB and Nas_{S1868} were optimized based on *E.*
338 *coli* codon bias and synthesized (GENEWIZ Co. Ltd., see below). The DNA fragment
339 of Nas_{F5053} was released by *Nde*I-*Xho*I digestion and cloned into the same sites of
340 pET28a to generate pSJTU1. The resulting plasmid was transferred into *E. coli* BL21
341 (DE3) for protein expression. After expression in 500 mL culture at 16 °C and 220 rpm
342 for 20 h following 100 μM isopropyl-β-D-thiogalactopyranoside (IPTG) induction (IPTG,
343 0.4 mM δ-aminolevulinic acid (ALA) and 0.2 mM (NH₄)₂Fe(SO₄)₂ were added when
344 OD₆₀₀ reached ~0.6), cells were harvested by centrifugation at 5,000 rpm at 4 °C. The
345 cell pellet was resuspended in 20 mL lysis buffer (25 mM HEPES, pH 7.5, 300 mM

346 NaCl, 5 mM imidazole, 10% glycerol) and lysed by ultra-sonication. The insoluble
347 debris was removed by centrifugation at 12,000 rpm, 4 °C for 1 h. The protein
348 supernatant was then incubated with 1 mL Ni-NTA sepharose for 1.5 h with slow,
349 constant rotation at 4 °C. Subsequently, the protein-resin mixtures were loaded into a
350 gravity flow column, and proteins were eluted with increasing concentrations of
351 imidazole (25 mM, 50 mM, 100 mM, 300 mM) in Buffer A (25 mM HEPES, pH 7.5, 300
352 mM NaCl, 10% glycerol). Purified proteins were then loaded into PD-10 desalting
353 columns and desalted using buffer B (25 mM HEPES, pH 7.5, 50 mM NaCl, 10%
354 glycerol) and concentrated by centrifugation using an Amicon Ultra-4 (GE Healthcare).
355 The purified proteins were evaluated by 12% acrylamide SDS-PAGE (**Supplementary**
356 **Fig. 15**).

357 Because NasbB and Nas_{S1868} could not be expressed as soluble proteins in *E. coli*,
358 we employed the *Mycobacterium* system for their expression. Firstly, a new plasmid
359 named pMS1 was developed by using the following method: the *pACE* gene was
360 amplified from the pMF406 vector with the primer pair Ami-for/Ami-rev and cloned into
361 the *Xba* I / *Bam*H I sites of the pMV261 vector to generate the plasmid pMV261-ACE.
362 Further, a gene fragment, obtained by annealing with the primers pair tev-for/tev-rev
363 was cloned into the *Bam*H I / *Eco*R I sites of pMV261-ACE, to yield the pMS1. Secondly,
364 the DNA fragments of these two P450s were cloned into the site between *Nde* I and
365 *Eco*R I of pMS1, to generate pSJTU2 and pSJTU3. These expression plasmids were
366 then electro-transformed into *Mycobacterium smegmatis* mc²155 for overexpression
367 of N-terminal 6× His-tagged fusion proteins. In 0.8 L of liquid culture, the cells were
368 grown at 30 °C in Lemoco media with 50 µg mL⁻¹ kanamycin to an OD₆₀₀ of 1.0-1.5.
369 The cells were then induced by 30 mM acetamide, 0.4 mM δ-aminolevulinic acid (ALA)
370 and 0.2 mM (NH₄)₂Fe(SO₄)₂ for 20 h at 30 °C. The cells were then harvested and the
371 subsequent steps were the same as for *E. coli* expression. Protein concentration was
372 determined by the Bradford method using a BSA calibration curve. The purified
373 proteins were stored at -80 °C and used for in vitro assays.

374 Sequences of synthetic P450s (restriction enzyme recognition sites are
375 underlined):

376 *nasbB*:
377 CATATGATTCGTCCGCAGCCGCATCGCAGTCCGGTTGACCCGTATAACCAAAGAAT
378 GCCGTACCGTGACCACCGCACCGGTTCCGCTGACCTTTCCTTTCCACGACTGG
379 AGTCAAGAGCTGAGTCCGCATCATGAACGTCTGCGCGAAGCAGATGCCCCGGT
380 GTGTCCGGTGGTGAGCGAATATAACGGCGATCGCCTGTGGCTGGTGACACGCT
381 ACGCCACCGCAAACGCCTGCTGGAGGATCGCCGTTTTAGCAGTACCGCCGCA
382 ATGGCACCTGGTGCACCGCGTCAGGAACCGGTGGAATTACGCGCACCGGGTAC
383 CACCGGTGACGGTGTGAGCGTTCTGCGCGAGGCAGGCCTGCGTACAGTGTTCA
384 CCGAAGGTTTAGGTCCGCGCGCAGCCCGTCGTCATGGTAAATGGCTGCGCGAT
385 CGTGCAGATACCTTACTGCGCGATGTTGCCGAGTGCGAAGGCCCGGTGGATCT
386 GGCAGCCGATTTTGCACAGCCGCTGGCCGTGGCAATGACAAGTCGCGTGCTGC
387 TGGGTGAACTGAGCACCGAAGAAGCCGCACTGTTACGTGATCGTACCGACCTG
388 GCCCTGCAGTTTTGTGGTGCAACCGCCGAAGAACAGCGCGGGCGGTCTGATTGA
389 TATTCATCGCTTTTTTACCGCCCATGCCCGCCGCTTAGCAGATGGTCCGGGTGAC
390 CACCTGCTGAAACGTCTGGCCGAAGCCCCGGCAGAAAATGGCCCGCTGGGTGA
391 TGCCGCCCTGAGTGAAATTGCCGCCCTGCTGCTGATTGCAGGCTTCCCGACCA
392 GTAGCGGCTTCCTGTGCGGTGCCCTGATCACACTGCTGCGCCATCCGGAAGCC
393 GTTGGTCGTCTGCGTCGCGATCCGGAAGTATTCTGACGCCGTGGAAGAACT
394 GCTGCGTCATACCCCGCTGAGCACCGGTGCCGCAAACGTATGGCCACCGAAG
395 ATGCCGATATTGACGGCGTTCGCATTCGCCGCGGTGAAGTGCCATGGTTAGCC
396 TGGAAGCCGCCAACCATGATCCTGACGCCTTCGATGATCCGGACAGTTTTCGTC
397 CGGAACGCCAGGGTCCGGGTCATCTGGGTTTTGGCCATGGCCCGAATTTTTGC
398 CCGGGTAATCGCCTGGCACGCTGTCTGATCGATGCCATGGTTCGTGCCGTTGCA
399 CGCCGTCCGGGTTTACACCTGACAGTGGGCCCGGAGGAGATCCGCTGGCATGA
400 AGGTCTGTTTTTCCGCCGTCCGAAAGCCATCCCGGCAAGCTGGTAACTCGAG

401 *nas_{S1868}*:
402 CATATGACAACCACCGCCACCCTGACCTATCCGTTTTACGATTGGAGCCAGGAG
403 CTGAGTCCGCGTTACGCCAGCTGCGTGCCAGTGATGCCCCGGTTTGCCCGGT
404 TGTGAGTGAAGGTACCGGCGATCATCTGTGGCTGGCAACCCGCTATGCCGCAG
405 CCGTTGAACTGCTGGAAGACCCTCGTCTGAGCAGCGAAGCCGCAATTGCAAGC

406 GGTGCACCTCGTCAGGAGCCGGTTGAACTGCGTGCACCTGGTACCCGTGCAGA
407 TGGTGTGCAATGCTGCGTGAAGCCGGCCTGCGCAGTGTCTGGCAGACGGTC
408 TGGGTCCGCGCGCAGTTCGTGCCATCAGGGCTGGATCAATGACTTAGCCGAA
409 ACCCTGATGAGCGCATTAGCAAGTCGCGAGGGCACCTTTGACCTGGCCGCCGA
410 TTTTGTGGAACCGCTGAGTAGTGCCCTGGTGAAGCCGTACCCTGCTGGGCGAAC
411 TGAGCGCAGATGAACGCGATCTGCTGGCCATTGTGCCGATACCGGTCTGCGCT
412 TCTGCGGTGTTACCCACGAAGAGCAGGTGCATGCCTTCACCCAGATGCATGAGT
413 TCTTCTGGAGCATGCCCGTCTGCTGGCAGGTACACCGGGTGAACACCTGCTG
414 AAAGTATCGCCGAAGCCCCGGTTGATCACGGCCCGTTAAGTATGAAGCCCTG
415 GCCGAAGCCGGTAGTCTGCTGGTGGTGGCAGGTTTTCCGACCAGCAGCGGCTT
416 TCTGTGCGGTGCACTGCTGACCTTACTGCGCCATCCGGATGCCGTTTACAGGAGCT
417 GCACGCCCATCCGGAACGCGTTCCTAGTGCCGTTGAGGAACTGCTGCGCTATAC
418 CCCGCTGAGCACCGGTAGCGTGAAACGCATGGCAACCGAAGATCTGGAAATCG
419 ACGGCGTGCGCATCAAAGTGGGTGAAGTGGTATGGTGAAGCCTGGAAGCCGTG
420 AATCATGACCCGGATGCCTTCGAAGATCCGGACGTGTTTCGTCCGGGTGCGGAA
421 GGCCCTATGCACTTTGGTTTTGGCCGCGGTGCCATTTTTGTCCGGGTAAACCGC
422 CTGGCCCGCTGTGTGATTGAAGCCACCGTTCGTGCAGTTGCACGTCGCCCGGG
423 TCTGCGTTTAGCAGTTGCCCGGAGGAAATCAGCTGGCATGAAGGCCTGTTCTT
424 TCGTCGCCCTCGTGCCATCCCGGCCACATGGTAAGCTT

425 *nas_{F5053}*:

426 CATATGACCACCACCGCAACCCTGACCTACCCGTTTCATGACTGGAGCCAGGAA
427 CTGAGCCCGCGTTATGCCAGCTGCGTGCAAGCGATGCACCGGTGTGTCCGGT
428 GGTGAGTGAAGGTACCGGTGACCCGCTGTGGCTGGTGAACGCTACGCCACCG
429 CCGTGAAACTGCTGGAAGATAGCCGCTTTAGCAGTGAAGCCGCACAGGCCAGT
430 GGTGACCGCGTCAGGAACCGGTGGAATTACGTGCCCCGGGTACACGCGGTGA
431 CGCCATTGCAATGCTGCGCGAGGCCGGTCTGCGTAGCGTTCTGGCCGACGGCT
432 TAGGTCCTCGTGCAAGTGCAGTGCAGCGTGCATCAGGGTTGGATCAACGACCTGGCCGAA
433 ACCCTGATGAGCGAATTAGCAAGCCGTGAAGGCACCTTTGACCTGGCCGCAGAT
434 TTTGTGGAACCGCTGAGTAGCGCCCTGGTGAAGTTCGTACACTGCTGGGCGAGCT
435 GAGCGCAGACGAACGCGATCTGCTGGCACATTGCGCCGATACCGGTCTGCGCT

436 TTTGCGGTGTGACACATGAAGAACAGGTGCACGCCTTCACCCAGATGCATGAGT
437 TCTTCCTGGAGCATGCACGTCGTCTGGCAGGTACCCCGGGTGAGCACCTGTAA
438 AACTGATTGCCGAGGCCCGGTTGATCAGGGTCCGCTGAGCGATGAGGCCCTG
439 GCAGAAGCAGGTAGCCTGCTGGTTGTGGCAGGCTTCCCGACCAGCAGCGGCTT
440 TCTGTGCGGTGCACTGCTGACCCTGCTGCGCCATCCGGATGCCGTGCAAGAAC
441 TGCATGCCACCCGGAACGTGTGCCTAGCGCAGTGGAAGAGCTGCTGCGTTATA
442 CCCCTCTGAGCACAGGCAGCGTGAAACGCATGGCCACCGAAGACCTGGAAATT
443 GACGGCGTGCGCATCAAAGCCGGTGAAGTGGTTATGGTGAGCCTGGAAGCAGT
444 GAACCATGATCCGGATGCCTTTGAGGATCCGGATGTTTTTCGCCCGGGTCGCGA
445 AGGTCCGATGCACTTTGGTTTTGGTCGTGGCCGTCATTTCTGTCCGGGCAATCG
446 CCTGGCACGTTGCGTGATTGAAGCAACCGTGCGTGACGTTGCACGTCGTCCGG
447 GTCTGCGTCTGGCAGTGGCACCCGGAAGAGATCAGCTGGCACGAGGGTCTGTTT
448 TTTCCGCGTCCGCGCGCCATTCCGGCAACATGGTAAGCTTGAATTC

449

450 **3.3. P450 enzyme assays**

451 The activities of wild-type and mutant P450s were assayed in HEPES buffer (50
452 mM HEPES, 100 mM NaCl, pH 7.5) containing 0.1 μ M purified P450s, 1 mM cW_L-PL,
453 1 μ M spinach ferredoxin (Fd), 1 μ M spinach ferredoxin reductase (FdR), 2 mM NADP⁺,
454 2 mM glucose and 2 mM glucose dehydrogenase (GDH). Expression and purification
455 of Fd, FdR, GDH were described previously³. The reaction was incubated at 4 °C. After
456 24 h, two times the volume of ethyl acetate was added to quench the reaction, followed
457 by sonication for 5 minutes. After the separation of aqueous and organic phases, the
458 ethyl acetate phase was transferred to a rotavapor to dry, which was re-dissolved in
459 HPLC-graded methanol. The resultant solution was filtered through a 0.45 μ M
460 membrane and subjected to analysis by UPLC-MS. A Diamonsil (C18, 2 μ m, 2.1 \times 50
461 mm, Shim-pack GIST) was used with a flow rate at 0.3 mL min⁻¹ and a PDA detector
462 over a 23 min gradient program with water (eluent A) and methanol (eluent B): T = 0
463 min, 40% B; T = 10 min, 40% B; T = 15 min, 70% B; T = 18 min, 40% B; T = 23 min,
464 40% B.

465

3.4. Scaled biocatalytic reaction and purification of NAS-B, ASP-A and NAS-E

Based on the whole-cell catalysis system we developed previously³, genes of *Nas*_{F5053} or its mutants, together with the plasmid pWHU2487 expressing Fd and FdR, were co-transferred into *E. coli* GB05-dir-T7. The resulting bacteria were inoculated in LB media (5 L) and grown to an OD₆₀₀ of 0.8-1.0 at 37 °C. After this, the cells were shifted to 18 °C, 220 rpm and supplemented with 100 μM isopropyl-β-D-thiogalactopyranoside (IPTG), 0.4 mM δ-aminolevulinic acid (ALA) and 0.2 mM (NH₄)₂Fe(SO₄)₂·6H₂O, for expression for additional 20 h. The cells were harvested by centrifugation at 5,000 rpm at 4 °C and resuspended in 200 mL M9 medium. Then, 100 mM cW_L-P_L (1 mL) was added in M9 media. After 48 h incubation at 18 °C, the reaction mixture was extracted with 400 mL ethyl acetate three times. The organic phase was transferred and dried by vacuum at a low temperature. Metabolites were subsequently redissolved by methanol and filtrated by a 0.45 μm membrane to remove particles. NAS-B and ASP-A were semi-prepared on a SHIMADZU LC-20A Prominence HPLC system using Venusil MP C18(2) (5 μm, 250 × 10 mm, Agela Technologies Inc.) at a flow rate of 3 mL min⁻¹. The MS and NMR data are summarized in **Supplementary Table 2-4** and the key HMBC and ROESY correlations in their structures are illustrated in **Supplementary Fig. 1-3**. The structures of NAS-B, ASP-A and NAS-E were deduced based on the NMR signals by following the strategy described previously³.

3.5. Site-directed mutagenesis of *Nas*_{F5053} and *NascB*

Rolling-circle PCR amplification was used to obtain all the site-directed mutants. Primers used for mutagenesis are all listed in **Supplementary Table 7**. Each PCR reaction (final volume 20 μL) containing 1 μL plasmid template, 1 μL primer pair (10 mM), 1 μL DMSO, 10 μL Primer Star DNA polymerase and 7 μL ddH₂O were initiated at 98 °C for 30 s to denature the template DNA, followed by 30 amplification cycles. Each amplification cycle consisted of 98 °C for 10 s, 55 °C for 30 s and 72 °C for 3.30 min. The PCR cycles were finished with an extension step at 72 °C for 10 min. After analyzing by agarose gel electrophoresis, 5 μL of each PCR product was transformed respectively into *E. coli* DH5α. The transformed cells were spread on a Luria-Bertani

496 (LB) plate containing kanamycin and incubated at 37 °C overnight. Two colonies from
497 each plate were grown and the plasmid DNA was isolated and verified by DNA
498 sequencing.

499 Overlap-PCR was used to introduce mutations on multiple residues simultaneously.
500 Taking fragment-7 of NascB as an example, two pairs of primers, nascB-F/nascB-7-R
501 and nascB-7-F/nascB-R, were used to prepare two NDA fragments, respectively,
502 based on the pWHU2485 DNA template. After purification by gel extraction kit, these
503 two fragments were used as a template to amplify the whole nascB gene, by using
504 nascB-F and nascB-R as primers. This PCR product was purified with the DNA gel
505 extraction kit, and then cloned into the pET28a vector by the Gibson assembly kit. The
506 plasmids were then isolated and sequenced to verify the desired mutations.

507

508 **3.6. Construction and screening of Nas_{F5053} mutant libraries**

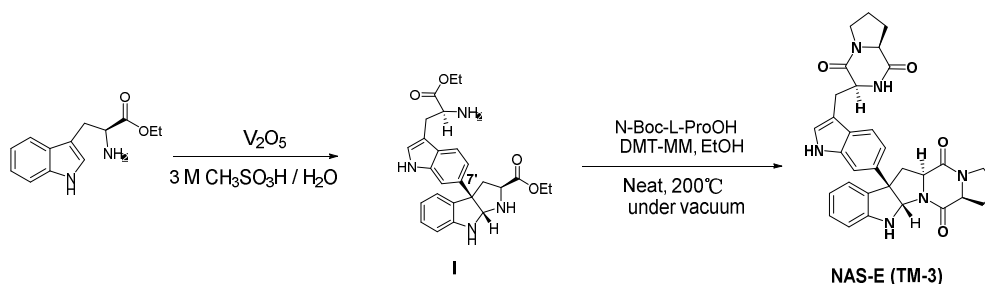
509 The 2-step PCR method developed by Reetz et al.⁵ was applied to construct the
510 Nas_{F5053} library. With the pET21a-Nas_{F5053} (wild-type) plasmid as the template, primers
511 F5053-SM-NNK-F and F5053-SM-NNK-R were used to amplify the megaprimers. After
512 all the megaprimers were confirmed by DNA agarose electrophoresis, they were used
513 directly to amplify the whole plasmid. Templates were removed by *Dpn* I digestion at
514 37 °C for 7 h, which was confirmed by electrophoresis. PCR amplicons (2 µL) were
515 directly transformed into 100 µL electrocompetent *E. coli* GB05-dir-T7, which contained
516 the plasmid pWHU2487 expressing Fd and FdR. After adding 900 µL LB media, the
517 cells were recovered at 37 °C for 1 h and then spread onto agar plates containing
518 kanamycin (50 µg mL⁻¹), ampicillin (100 µg mL⁻¹) and apramycin (50 µg mL⁻¹).

519 After incubating for 14 h at 37 °C, 400 individual colonies were picked from the
520 plate and inoculated into 500 µL of LB in a 2 mL 96-well plate. This plate was grown
521 for 12-16 h at 37 °C and 220 rpm. 100 µL portions of each culture were transferred to
522 a new 0.5 mL 96-well plate containing 100 µL of sterile glycerol (40 %, v/v) for stock.
523 The rest of the bacteria were supplemented with 100 µmol IPTG, 400 µmol ALA and
524 200 µmol (NH₄)₂Fe(SO₄)₂·6H₂O and continued to be expressed at 18 °C and 220 rpm
525 for 20 h. The cells were harvested by centrifugation at 3,000 rpm at 4 °C and

526 resuspended in 400 μ L M9 media. Then, 1 μ L of cW_L-P_L (100 mM) was added to the
527 M9 media. After 48 h incubation at 18 °C, the reaction mixture was extracted with 1 mL
528 ethyl acetate three times. The organic phase was transferred and dried by vacuum at
529 a low temperature. Metabolites were subsequently redissolved by methanol and
530 filtrated by a 0.45 μ m membrane to remove particles. The activities of each mutants
531 were analyzed by UPLC-MS, using the same condition mentioned above.

532

533 3.7. Synthesis of NAS-E



534

535 According to the method developed by Hayato Ishikawa⁶, V_2O_5 (50.2 mg, 0.28
536 mmol) was added to an aqueous CH_3SO_3H solution (10 mL, 3 M), and the suspended
537 mixture was stirred at room temperature in an open flask until the solution became
538 clear yellow. L-tryptophan ethyl ester (115.9 mg, 0.50 mmol) was added to the solution
539 of V_2O_5 at 0 °C. The reaction mixture was stirred for 8 h at 0 °C in an open flask. The
540 reaction mixture was slowly quenched with excess amount of aqueous 28% NH_4OH
541 solution at 0 °C. Then, the reaction was extracted three times with ethyl acetate. The
542 combined organic layer was dried over $MgSO_4$, and concentrated under reduced
543 pressure. Flash chromatography (SiO_2 , 5% MeOH/ $CHCl_3$ to 10 % MeOH/ $CHCl_3$ and
544 20% MeOH/ EtOAc) provided the desired intermediate I: 1H NMR (400 MHz, $CDCl_3$) δ
545 8.02 (s, 1H), 7.46 (d, $J = 9.0$ Hz, 1H), 7.19 (s, 1H), 7.08 (d, $J = 9.0$ Hz, 1H), 7.04 (t,
546 $J = 7.8$ Hz, 1H), 6.98 (d, $J = 7.5$ Hz, 1H), 6.95 (s, 1H), 6.67 (t, $J = 7.5$ Hz, 1H), 6.56 (d,
547 $J = 7.5$ Hz, 1H), 5.18 (s, 1H), 4.20 (m, 4H), 3.78 (m, 2H), 3.18 (dd, $J = 4.8, 14.8$ Hz, 1H),
548 2.98 (m, 1H), 2.80 (m, 1H), 2.59 (t, $J = 11.8$ Hz, 1H), 1.25 (m, 6H); ^{13}C NMR (101 MHz,
549 $CDCl_3$) δ 175.1, 173.4, 149.6, 138.2, 136.0, 133.2, 128.0, 125.8, 124.9, 122.9, 119.2,
550 119.1, 118.0, 111.0, 109.4, 108.6, 85.9, 63.6, 61.3, 61.1, 60.6, 55.1, 46.0, 30.3, 14.2,
551 14.2.

552 To a solution of intermediate I (50 mg, 0.11 mmol) and N-(t-butoxycarbonyl)-L-
553 proline (Boc-L-Pro, 47 mg, 0.22 mmol) in EtOH (5 mL), 4-(4, 6-dimethoxy-1,3,5-triazin-
554 2-yl)-4-methylmorpholinium chloride (DMT-MM, 60 mg, 0.22 mmol) was added at 0 °C
555 in an open flask (50 mL round-bottom flask). The resulting mixture was stirred for 4 h
556 at 0 °C, before removing the solvent under reduced pressure. The crude material was
557 directly heated at 200 °C under vacuum (0.1 mbar) for 15 min, before quenching with
558 excess amount of aqueous 28% NH₄OH solution. The aqueous layer was extracted
559 three times with 5% MeOH/ CHCl₃. The combined organic layer was washed with brine,
560 dried over MgSO₄, and concentrated under reduced pressure. Flash chromatography
561 (SiO₂, 2 % MeOH/ saturated NH₃/ CHCl₃) provided NAS-E (TM-3) (10.0 mg) as white
562 amorphous powder (**Supplementary Fig. 10**): ¹H NMR (400 MHz, DMSO-*d*₆) δ 10.79
563 (s, 1H), 7.65 (s, 1H), 7.50 (d, *J* = 8.4 Hz, 1H), 7.23 (s, 1H), 7.15 (d, *J* = 8.4 Hz, 1H),
564 7.14 (d, *J* = 2.7 Hz, 1H), 7.07 (dd, *J* = 1.5, 8.4 Hz, 1H), 6.99 (m, 1H), 6.66 (d, *J* = 3.0
565 Hz, 1H), 6.64 (d, *J* = 2.7 Hz, 1H), 6.61 (m, 1H), 5.56 (s, 1H), 4.31 (d, *J* = 7.9 Hz, 1H),
566 4.26 (m, 1H), 4.17 (m, 1H), 4.05 (m, 1H), 3.34 (m, 2H), 3.25 (m, 2H), 3.20 (m, 1H),
567 3.04 (m, 1H), 3.00 (m, 1H), 2.65 (m, 1H), 2.13 (m, 1H), 1.96 (m, 2H), 1.80 (m, 2H),
568 1.60 (m, 2H), 1.38 (m, 1H); ¹³C NMR (101 MHz, DMSO-*d*₆) δ 169.2, 166.2, 165.6,
569 165.4, 149.4, 136.9, 136.0, 132.5, 128.3, 126.1, 124.9, 124.0, 119.0, 118.2, 116.4,
570 109.6, 109.2, 108.1, 81.5, 60.2, 59.8, 58.9, 58.5, 55.2, 44.7, 27.7, 27.4, 25.8, 22.6,
571 21.9.

572

573 **3.8. Cloning, expression, crystallization and crystal structure determination of** 574 **Nas_{F5053} and its mutants**

575 The first 5 amino acids (MTTTA) of Nas_{F5053} were confirmed to have no effect on
576 enzyme activity and were thus removed as presumably flexible, for potential benefit in
577 crystallization. With the first 5 amino acids removed, the Nas_{F5053} gene was amplified
578 with the primer pair F5053-Xray-For/F5053-Xray-Rev and cloned into pSrtA9 through
579 ligation-independent cloning⁷. Using New England Biolabs Q5 site-directed
580 mutagenesis kit, the Nas_{F5053}-Q65I-A86G mutant was prepared through two
581 successive rounds of single mutagenesis (the first primer pair: F5053-Q65I-For/

582 F5053-Q65I-Rev; the second primer pair: F5053-A86G-For/ F5053-A86G-Rev-). The
583 Nas_{F5053}-S284A-V288A mutant was constructed with the primer pair Nas_{F5053}-S284A-
584 V288A-For/Nas_{F5053}-S284A-V288A-Rev. The resulting constructs were confirmed by
585 standard Sanger sequencing at the Australian Genome Research Facility (AGRF).
586 Nas_{F5053} was expressed as an N-terminal fusion with SrtA, i.e. His6-SrtA-Nas_{F5053}. The
587 expression and purification were performed as previously reported⁶ and further
588 polished by running through a Superdex S200 gel filtration column with 20 mM HEPES,
589 100 mM NaCl, pH 7.5. As evaluated by SDS-PAGE, the elution fractions containing
590 pure Nas_{F5053} protein were pooled and concentrated to 7 mg mL⁻¹ for protein
591 crystallization, using centrifugal filter units (Amicon MWCO 30 kDa, Millipore). The
592 concentration of 7 mg mL⁻¹ was determined by absorbance at A₂₈₀ and a theoretical
593 extinction coefficient. 1 mM DTT was added to the final Nas_{F5053} protein solution. The
594 yield of Nas_{F5053} was approximately 1-2 mg L⁻¹ LB medium. Two extra amino acids, i.e.
595 Gly and Ser, were left at the N-terminus of Nas_{F5053}.

596 Initial crystals were obtained in 0.2 M CaCl₂, 20% (w/v) polyethylene glycol (PEG)
597 3350 at 20 °C, using the hanging drop vapor diffusion technique with the addition of 5%
598 glycerol to the protein stock. The initial crystals were subsequently crushed for seeding
599 by using the Seed Bead Kit (Hampton Research). The best crystals were obtained
600 using the micro-seeding technique in 0.2 M CaCl₂, 22 % (w/v) PEG 3350, pH 7.5 at
601 4 °C. Substrate-bound protein crystals were obtained by soaking the substrate-free
602 crystals in the mother liquor containing 2.5 mM cW_L-P_L (diluting from 50 mM stock
603 solution in DMSO) for 24 h.

604 Crystals were mounted onto CryoLoops (Hampton Research) and soaked in a
605 cryoprotection solution containing 0.2 M CaCl₂, 22 % (w/v) PEG 3350, and 20% (v/v)
606 glycerol prior to flash-cooling in liquid nitrogen. For the substrate-bound protein
607 crystals, the cryoprotection solution also contained 2.5 mM cW_L-P_L. X-ray diffraction
608 data were collected at the Australian Synchrotron MX beamlines. The collected data
609 were indexed and integrated using *XDS*⁸ and scaled and merged using *Aimless*⁹. A
610 partial initial model of the *ligand-free* structure was obtained by the molecular
611 replacement technique with *Phaser* in *Phenix*¹⁰ using the crystal structure of CYP121

612 from *Mycobacterium tuberculosis* (PDB ID **5WP2**) as the search model¹¹. The initial
613 model was improved by using the *Morph Model* tool in *Phenix*¹² and manually modified
614 in *COOT*¹³. The substrate-bound structure was solved by the molecular replacement
615 technique using the *ligand-free* structure as the search model. The structures were
616 iteratively refined using *Phenix.Refine*¹⁴ and manually modified in *COOT*.

617

618 **3.9. Molecular dynamics simulations**

619 **System preparation.** Molecular dynamics simulations were performed based on the
620 X-ray structures we determined in this study, including the wild-type Nas_{F5053}/cW_L-P_L
621 (PDB ID 6VXV), Nas_{F5053}-Q65I-A86G/cW_L-P_L (PDB ID 6VZA), and Nas_{F5053}-S84A-
622 V288A/cW_L-P_L (PDB ID 6VZB). Parameters for substrates and the heme group for the
623 molecular dynamics simulations were generated within the antechamber module of
624 AMBER 18, using the general AMBER force-field, with partial charges set to fit the
625 electrostatic potential generated at the B3LYP/6-31G(*d*) level by the restrained
626 electrostatic potential model. The charges were calculated according to the Merz–
627 Singh–Kollman scheme, using Gaussian 09. Amino acid protonation states were
628 predicted using the H++ server (<http://biophysics.cs.vt.edu/H++>).

629 **Molecular dynamics simulation details.** The wild-type enzyme (PDB ID 6VXV) and
630 variants were solvated in a pre-equilibrated truncated cuboid box with a 10 Å buffer of
631 TIP4PEW water molecules, using the AMBER 18 leap module¹⁵, resulting in the
632 addition of approximately 9,000 solvent molecules. The system was neutralized by the
633 addition of explicit counterions (Na⁺ and Cl⁻); in particular, we added 6 Na⁺ counter ions.
634 MD simulations were performed with the sander.MPI of Amber19 program using the
635 Amber ff14SB force field for protein and GAFF2 for substrate¹⁶. The partial charges of
636 the heme and the substrates were obtained at the B3LYP level of theory and LANL2DZ
637 basis set for Fe and 6-31G for C, H, O, N, S atoms by Gaussian 09¹⁷. A two-stage
638 geometry optimization approach was performed. The first stage minimizes the
639 positions of solvent molecules and ions, imposing positional restraints on solute by a
640 harmonic potential with a force constant of 500 kcal mol⁻¹ Å⁻², and the second stage is
641 an unrestrained minimization of all of the atoms in the simulation cell. The systems are

642 gently heated using six 50 ps steps, incrementing the temperature 50 K each step (0–
643 303 K, 30°C) under constant volume and periodic boundary conditions. Water
644 molecules were treated with the SHAKE algorithm, such that the angle between the
645 hydrogen atoms is kept fixed. Long-range electrostatic effects were modelled using the
646 particle mesh Ewald method. An 8 Å cutoff was applied to Lennard-Jones and
647 electrostatic interactions. Harmonic restraints of 10 kcal mol⁻¹ were applied to the
648 solute and the Langevin equilibration scheme was used to control and equalize the
649 temperature. The time-step was kept at 1 fs during the heating stages, allowing
650 potential in homogeneities to self-adjust. Each system was then equilibrated without
651 restraints for 2 ns, with a 2 fs time-step at a constant pressure of 1 atm and temperature
652 of 300 K. After the systems were equilibrated in the NPT ensemble, 100 ns molecular
653 dynamics simulations were performed under the NVT ensemble and periodic boundary
654 conditions. The RMSDs of all the simulations are show in **Supplementary Fig. 14**.

655

656 **3.10. UV-Vis titration and determination of the binding constants of cW_L-P_L to** 657 **Nas_{F505}, Nas_{F5053}-Q65I-A86G or Nas_{F5053}-S284A-V288A.**

658 We used a double-beam UV-2600 (SHIMADZU) spectrophotometer and 1-cm
659 pathlength quartz cells to measure UV-Vis absorbance of 2 μM Nas_{F5053} or its mutants.
660 Spectral titration with cW_L-P_L was performed at 15 °C with reference to the reported
661 procedures^{18,19}. Difference spectra were generated by subtracting the spectrum
662 obtained without cW_L-P_L from that recorded for each cW_L-P_L concentration. Thereafter,
663 the absorbance variations were calculated from the difference spectra ($\Delta A_{387} - \Delta A_{417}$)
664 and were plotted against the relevant cW_L-P_L concentrations. The binding constants
665 (K_s) were extracted from fitting the plotted data points to the following equation:

$$666 \quad \Delta A = (\Delta A_{\max} \cdot [S]) / (K_s + [S])$$

667 where ΔA is the absorbance difference $\Delta A_{387} - \Delta A_{417}$, ΔA_{\max} is the maximum reachable
668 value of ΔA at saturating substrate concentrations, [S] is the substrate concentration
669 and K_s is the apparent binding constant. K_s were reported as means of four
670 independent experiments.

671

672 **4. Supplementary References**

673

- 674 1. Yu, H. & Li, S.-M. Two cytochrome P450 enzymes from *Streptomyces* sp. NRRL
675 S-1868 catalyze distinct dimerization of tryptophan-containing cyclodipeptides. *Org.*
676 *Lett.* **21**, 7094-7098 (2019).
- 677 2. Fan, X.-Y., Ma, H., Guo, J., Zhu, Z.-Q., Guo, S.-Q. & Zhao, G.-P. Development of
678 mycobacterial inducible expression system and application for immunological
679 diagnostics on tuberculosis. *Chin. J. Microbiol. Immunol.* **29**, 1104-1109 (2009).
- 680 3. Tian, W., Sun, C., Zheng, M., Harmer, J. R., Yu, M., Zhang, Y., Peng, H., Zhu, D.,
681 Deng, Z., Chen, S.-L., Mobli, M., Jia, X. & Qu, X. Efficient biosynthesis of
682 heterodimeric C-3-aryl pyrroloindoline alkaloids. *Nat. Commun.* **9**, 4428 (2018).
- 683 4. Sambrook, J., Russell, D.W. Molecular cloning: a laboratory manual, 3rd ed. Cold
684 Spring Harbor Laboratory Press, New York, (2001).
- 685 5. Li, A., Acevedo-Rocha C. G. & Reetz M. T., Boosting the efficiency of site-saturation
686 mutagenesis for a difficult-to-randomize gene by a two-step PCR strategy. *Appl.*
687 *Microbiol. Biotechnol.* **102**, 6095-6103 (2018).
- 688 6. Tadano, S., Sugimachi, Y., Sumimoto, M., Tsukamoto, S. & Ishikawa, H. Collective
689 synthesis and biological evaluation of tryptophan-based dimeric diketopiperazine
690 alkaloids. *Chem. Eur. J.* **22**, 1277-1291 (2016).
- 691 7. Jia, X., Crawford, T., Zhang, A. H. & Mobli, M. A new vector coupling ligation-
692 independent cloning with sortase a fusion for efficient cloning and one-step
693 purification of tag-free recombinant proteins. *Protein Expr. Purif.* **161**, 1-7 (2019).
- 694 8. Kabsch, W. XDS. *Acta Cryst.* **D66**, 125-132 (2010).
- 695 9. Evans, P. R. & Murshudov, G. N. How good are my data and what is the resolution?
696 *Acta Cryst.* **D69**, 1204-1214 (2013).
- 697 10. Adams, P. D., Afonine, P. V., Bunkóczi, G., Chen, V. B., Davis, I. W., Echols, N.,
698 Headd, J. J., Hung, L.-W., Kapral, G. J., Grosse-Kunstleve, R. W., McCoy, A. J.,
699 Moriarty, N. W., Oeffner, R., Read, R. J., Richardson, D. C., Richardson, J. S.,
700 Terwilliger T. C. & Zwart P. H. PHENIX: a comprehensive Python-based system for
701 macromolecular structure solution. *Acta Cryst.* **D66**, 213-221 (2010).
- 702 11. Fielding, A. J., Dornevil, K., Ma, L., Davis, I. & Liu, A. Probing ligand exchange in
703 the P450 enzyme CYP121 from *Mycobacterium tuberculosis*: dynamic equilibrium
704 of the distal heme ligand as a function of pH and temperature. *J. Am. Chem. Soc.*
705 **139**, 17484-17499 (2013).
- 706 12. Terwilliger, T. C., Read, R. J., Adams, P. D., Brunger, A. T., Afonine P. V. & Hung.
707 L.-W. Model morphing and sequence assignment after molecular replacement.
708 *Acta Cryst.* **D69**, 2244-2250 (2013).

- 709 13. Emsley, P., Lohkamp, B., Scott, W. G. & Cowtan, K. Features and development of
710 Coot. *Acta Cryst.* **D66**, 486-501 (2010).
- 711 14. Afonine, P. V., Grosse-Kunstleve, R. W., Echols, N., Headd, J. J., Moriarty, N. W.,
712 Mustyakimov, M., Terwilliger, T. C., Urzhumtsev, A., Zwart P. H. & Adams, P. D.
713 Towards automated crystallographic structure refinement with phenix.refine. *Acta*
714 *Cryst.* **D68**, 352-367 (2012).
- 715 15. Salomon-Ferrer, R., Case, D. A. & Walker, R. C. An overview of the Amber
716 biomolecular simulation package. *Wires Comput. Mol. Sci.* **3**, 198-210 (2013).
- 717 16. Maier, J.A., Martinez, C., Kasavajhala, K., Wickstrom, L. & Hauser K.E.,
718 Simmerling, C. ff14SB: Improving the accuracy of protein side chain and backbone
719 parameters from ff99SB. *J. Chem. Theory Comput.* **11**, 3696-3713 (2015).
- 720 17. Li, P. & Merz, K. M. Metal ion modeling using classical mechanics. *Chem. Rev.* **117**,
721 1564-1686 (2017).
- 722 18. Schenkman, J., Jansson, I. Spectral analyses of cytochromes P450. *Methods Mol.*
723 *Biol.* **320**,11–18 (2006).
- 724 19. Belin, P. et al. Identification and structural basis of the reaction catalyzed by
725 CYP121, an essential cytochrome P450 in Mycobacterium tuberculosis. *Proc. Natl.*
726 *Acad. Sci. U. S. A.* **106**, 7426-7431 (2009).
- 727